Submitted to Advances in Nuclear
Science and Technology

UCRL-20506
Preprint

TECHNICAL BASIS OF THE GAS CENTRIFUGE

Donald R. Olander

January 1971

AEC Contract No. W-7405-eng-48

LAWRENCE RADIATION LABORATORY
UNIVERSITY of CALIFORNIA BERKELEY

DISCLAIMER

UCRL-20506

TECHNICAL BASIS OF THE GAS CENTRIFUGE[†]

Donald R. Olander

Department of Nuclear Engineering
University of California
and the
Inorganic Materials Research Division
Lawrence Radiation Laboratory
Berkeley, California 94720

[†]Part of this work performed under the auspices of the Atomic Energy Commission.

TABLE OF CONTENTS

I. INTRODUCTION

A. Economic Incentives

The gas centrifuge or ultracentrifuge is a device which separates the isotopes of uranium by the action of a centrifugal force field some 10^5 times greater than gravity. Ultracentrifuges of various types were investigated extensively during the Second World War as a possible means of separating uranium isotopes for nuclear weapons. With the decision to employ the gaseous diffusion process as the sole supplier of enriched uranium, interest in the centrifuge isotope separation method diminished considerably in the United States. Because of the large investment in the equipment and technology of the gaseous diffusion process, American planning for future enriched uranium requirements for nuclear reactors does not seriously consider the gas centrifuge as a competitor.

However, the rapid growth of nuclear reactor capacity in Western Europe and Japan, which do not have large gaseous diffusion capabilities, has generated considerable interest in the gas centrifuge as the principal means of producing slightly enriched uranium for the nuclear power industry. Perhaps the most attractive feature of the gas centrifuge process to these countries is the relatively low electric power requirements. The three American gaseous diffusion plants, when operated at full load, consume as much power as one third of the electrical generating capacity of the West German Federal Republic. Preliminary estimates

suggest that the cost of electricity in the gas centrifuge process contributes ∿10% to the cost of separative work, compared to nearly 50% in the gaseous diffusion process. The cost of electricity in Europe is higher than in the United States, so that an isotope separation method less prodigal of electric power is highly desirable. In addition, gas centrifuge plants can be operated economically on a much smaller scale than the size of an optimum gaseous diffusion facility.

On the other hand, scale-up of a gas centrifuge plant is not simply a matter of increasing the size of individual separating units, since the performance and mechanical reliability of a gas centrifuge are critically dependent upon its size. Isotope separation plants satisfying European demands for enriched uranium would require very large numbers of individual centrifuges, perhaps as many as several million, each operating at rotational speeds greater than 50,000 RPM. Questions of reliability and life-time, which significantly affect product cost, can only be answered by plant-scale demonstration of the process. However, the gas centrifuge process is sufficiently promising to have prompted the British, Dutch and West German governments to form a company to bring the process to the stage of commercial exploitation (1,2).

B. Scope of the Review

There are many aspects to the use of the gas centrifuge for separating the isotopes of uranium. In the present review, the economic and technological questions touched

upon above will not be explored further. Additional discussion of the economic and political considerations may be found in refs. 3-8. Engineering aspects, such as rotor design, mechanical stability, and material selection are treated in refs. 9-16.

The present review is restricted to an analysis of the performance of the gas centrifuge, based primarily upon the equations of diffusion and hydrodynamics which govern the phenomena occurring in the device. In addition, only a particular type of gas centrifuge will be discussed. During the Manhattan Project, three types of centrifuges were investigated: the evaporative, concurrent, and countercurrent modifications. Only the last of these is seriously considered for large scale application, primarily because the flow pattern in this mode of operation acts to multiply the simple process effect many times. High separation factors can be achieved in a single unit, or in effect, a single countercurrent centrifuge behaves like a miniature isotope separation cascade.

Distinction must be made between two methods of establishing the countercurrent flow in the spinning rotor or "bowl" of the centrifuge. These methods are illustrated in Figs. 1 and 2. In the Beams device (17) (shown in Fig. 1), the countercurrent is established by streams introduced at opposite ends and different radial positions. Reflux and flow are maintained by pumps outside the device, so that the countercurrent is said to be external.

Figure 2 shows the ZG3 centrifuge of Groth (9).

In this configuration, countercurrent flow is due to thermal convection set up by maintaining the top cover of the rotor at a slightly higher temperature than the bottom cover. This type of countercurrent centrifuge is called a thermally driven or internal countercurrent device. The feed to the centrifuge enters the bowl from a small tube on the axis. To avoid mixing of streams of different compositions (which is anathema in all isotope separation methods), the axial location of the feed point is chosen so that the feed composition is the same as the composition in the device established by the combined centrifugal and axial circulation processes. In the thermally driven centrifuge, the magnitude of the circulating flow (represented by the sum of the "up" and "down" flows) can be adjusted independently of the feel flow rate or throughput. This ability to select the "reflux ratio" by simply adjusting internal temperatures represents a degree of flexibility not available in the centrifuge of Fig. 1, where refluxing is performed by an external pump. Only the thermally driven centrifuge is presently under consideration for large scale separation of uranium isotopes, and only this type will be discussed here.

The gas centrifuge may be analyzed in two distinct steps: (1) the <u>hydrodynamic</u> analysis seeks to determine the nature and magnitude of the gas flow within the rotor. (2) The <u>separative</u> analysis determines the manner in

which the centrifuge performs as an isotope separator.

Although the separative properties are dependent upon the hydrodynamics of the device, considerable progress can be made by analyzing the separative behavior under the assumption that the flow patterns are known. Such a procedure delineates the features of the hydrodynamics which are essential to the understanding of the isotope separating capability of the centrifuge. The hydrodynamic analysis considers the behavior of a single component working gas, while the separative analysis explicitly regards the fluid as a two component isotopic mixture. In this review, the separative behavior is considered in Sec. II and the hydrodynamics in Sec. III.

C. Separative Properties of a Centrifuge

The two parameters which are obtained from the separative analysis are the separation factor (or simple process factor) α and the separative power δU of a single centrifuge. These two properties are related to the design features of the centrifuge, the physico-chemical properties of the process gas (uranium hexafloride), the flow pattern, and controllable variables such as the throughput and the cut.

The importance of the separation factor and the separative power can best be appreciated by regarding a single centrifuge as a black box, or separating unit, which possesses a small number of formal properties by which its efficiency as an isotope separator can be gauged. Fig. 3 shows such a separating unit. Each unit receives a

feed of composition x_F and flow rate (or throughput) L and delivers a product stream (or heads stream) of composition x_P and flow rate P and a waste (or tails) stream of composition x_W and flow rate W. The cut of the separating unit is defined by:

$$\theta = P/L \tag{1}$$

A material balance over the separating unit on the desired isotope (the one referred to by the designation of isotope fraction x) yields:

$$x_F = \theta x_P + (1-\theta)x_W \tag{2}$$

The separation factor is defined by:

$$\alpha = \frac{x_P/(1-x_P)}{x_W/(1-x_W)} \tag{3}$$

When defined by Eq. (3), the separation factor is independent of composition but may depend upon the throughput L and the cut θ. A large value of α is desirable, but is not the only important characteristic of the separating unit. For example, a particular device may produce a large separation factor only at very small throughput. In order to process a certain amount of feed material, a large number of separating units may be required even though α is large. Consequently, a separating unit which exhibits a relatively modest separation factor but does so at a reasonably large

flow rate may be more desirable from the point of view of cascade design.

Quantitatively, the dependence of the efficiency of a separating unit on the combined effects of throughput and enrichment is characterized by the separative power of the unit. To describe this feature of the separating unit, the work which the device does on the fluid it processes is viewed as increasing the "value" of the material. The value of a unit amount of material of isotopic composition x is denoted by V(x), which is termed the value function. The separative power of the unit is defined as the increase in the value of the streams leaving the unit over the feed stream. A "value balance" can be made in a manner analogous to a material balance. For the separating unit shown in Fig. 3, this balance yields:

$$\delta U = \theta LV(x_P) + (1-\theta)LV(x_W) - LV(x_F) \qquad (4)$$

Both the separative power δU and the form of the value function V(x) can be determined by a single requirement: that δU be independent of isotopic composition of the streams entering and leaving the unit. Subsequent analysis is considerably simplified (and yet remains sufficiently accurate for our purposes) if only "close separation" processes are considered. By close separation we mean that the elementary effect of each separating unit is quite small, or that the compositions of all streams entering

and leaving the unit differ but little from each other. This condition is fulfilled if the separation factor α is close to unity. Under the close separation restraint, the value functions $V(x_p)$ and $V(x_W)$ may be obtained from Taylor series expansions about the feed composition:

$$V(x_p) = V(x_F) + \left(\frac{dV}{dx}\right)(x_p-x_F) + \frac{1}{2}\left(\frac{d^2V}{dx^2}\right)(x_p-x_F)^2 \qquad (5)$$

Use of Eqs. (2) and (5) (plus the analog of Eq. (5) for $V(x_W)$) in Eq. (4) yields:

$$\delta U = \frac{1}{2}L\theta(1-\theta)(x_p-x_W)^2\left(\frac{d^2V}{dx^2}\right) \qquad (6)$$

In the close separation case, the defining equation for the separation factor, Eq. (3), may be simplified by neglecting $\alpha-1$ compared to unity:

$$x_p-x_W = (\alpha-1)x(1-x) \qquad (7)$$

Since the compositions of all three streams entering or leaving the unit are close to each other, it is immaterial whether x_F, x_W, or x_p is used as the composition variable on the right hand side of Eq. (7). It has been denoted simply by x.

Combining the preceding two equations results in:

$$\delta U = \frac{1}{2}\theta(1-\theta)(\alpha-1)^2L[x(1-x)]^2\left(\frac{d^2V}{dx^2}\right) \qquad (8)$$

In order to satisfy the requirement that δU be composition independent we must set

$$\frac{d^2V}{dx^2} = \frac{1}{[x(1-x)]^2} \tag{9}$$

Eq. (9) can be integrated directly. With the auxillary specifications $V(0.5) = (dV/dx)_{0.5} = 0$ (which are chosen for convenience and do not affect the basic properties of the value function), integration yields:

$$V(x) = (2x-1)\ell n\left(\frac{x}{1-x}\right) \tag{10}$$

The concentration-independent separative power of a single separating unit is thus seen to be:

$$\delta U = \frac{1}{2}\theta(1-\theta)(\alpha-1)^2 L \tag{11}$$

D. The Ideal Cascade

A large scale isotope separations plant consists of a large number of separating units arranged in the form of an ideal (or no-mixing) cascade. An ideal cascade is sketched in Fig. 4. To differentiate the process streams entering and leaving the cascade from those pertaining to a single separating unit, the flow rates in Fig. 4 are written in script and the isotope fractions are denoted by X.

The properties of an ideal cascade (irrespective of the nature of the separating units of which it is composed)

are described in the book by Cohen (18). The height of the cascade (from the waste end to the product end) is proportional to the number of stages required to effect the desired separation. Provided that the separation factor is independent of composition and close to unity (the close separation approximation), the total number of stages in the cascade is:

$$\text{number of stages} = \left(\frac{2}{\alpha-1}\right) \ell n \left[\frac{X_P/(1-X_P)}{X_W/(1-X_W)}\right] \tag{12}$$

A stage may be represented by a horizontal line in the diagram of Fig. 4. The width of the cascade at any stage is a measure of the number of separating units at that particular point. All separating units in a given stage receive the same feed and produce the same heads and tails streams. The total area contained within the diagram of Fig. 4 is proportional to the total number of separating units in the cascade. It can be shown that the total interstage flow rate in a close separation, ideal cascade whose separating units operate at a cut θ is given by[1]:

$$J = \frac{2}{(\alpha-1)^2 \theta(1-\theta)} U \tag{13}$$

where, by analogy to Eq. (4), U is the separative capacity of the entire cascade:

$$U = \mathcal{P} V(X_P) + \mathcal{W} V(X_W) - \mathcal{F} V(X_F) \tag{14}$$

[1]Footnotes are collected at the end.

Division of Eq. (11) into Eq. (13) shows that J/L, which is the number of separating units in the cascade, is:

$$\text{number of separating units} = J/L = U/\delta U \qquad (15)$$

Between them, α and δU determine all of the properties of the cascade. If U is regarded as a design specification of the cascade, δU fixes the number of units required by Eq. (15). The separation factor α determines the number of stages by Eq. (12). The taper of the cascade is also determined by these two properties of the individual separating units.

It is desirable that both α and δU be large. The larger δU, the smaller the number of units in the cascade, which is obviously advantageous. If α is large, the cascade shown in Fig. 4 is short and squat, since the number of stages required for the overall separation is small. Each stage consists of a large number of separating units in parallel and much of the recycling between stages which is necessary for small-α cascades is avoided. Problems of cascade operation are reduced to the extent that separating units can be arranged in parallel rather than in series. However, minimization of the number of separating units in the cascade is the dominant consideration, and if a choice must be made, it is preferable to design for maximum δU rather than maximum α.

II. SEPARATIVE PROPERTIES OF THE GAS CENTRIFUGE

This section is concerned with the theoretical description of the manner in which a thermally driven gas centrifuge produces a separation of the components of a binary isotopic gas mixture. The object is to determine the separation factor α and the separative power δU of the machine, with particular emphasis given to the dependence of these properties on controllable parameters such as internal flow rate, throughput, and the cut.

The basic conservation equations in a one component system are those of mass (overall continuity), momentum, and energy. In Sec. III, these equations are utilized to describe the fluid velocity field in the gas contained in the centrifuge. In the present analysis, the fluid velocity, denoted by the vector $\underline{v}$, is assumed known.

A. Species Continuity Equation

In fluids composed of two components (in the present case, different isotopes), an additional conservation relation is applicable; the "species continuity equation" describes conservation of one of the two components of the mixture.[2] In a mixture of components A and B, the continuity equation for species A is (19):

$$\frac{\partial C_A}{\partial t} + \nabla \cdot \underline{N}_A = 0 \qquad (16)$$

where C_A is the molar concentration of component A(moles/cm^3), ∇ is the gradient operator, and $\underline{N}_A$ is the vector molar flux

of component A in moles/cm^2-sec. $\underline{N}_A$ consists of two parts: a diffusive (or separative) term $\underline{J}_A$ which describes the flux of A relative to the average velocity of the mixture and a convective (or non-separative) term which describes the flux of A due simply to the bulk motion of the fluid:

$$\underline{N}_A = \underline{J}_A + C_A\underline{v} \tag{17}$$

where $\underline{v}$ is the vector velocity of the bulk fluid.[3]

Substituting (16) into (17) yields:

$$\frac{\partial C_A}{\partial t} + \nabla\cdot(C_A\underline{v}) = -\nabla\cdot\underline{J}_A \tag{18}$$

In the case of the gas centrifuge, two components of $\underline{J}_A$ are important: the contribution $\underline{J}_A^{(m)}$ due to ordinary molecular diffusion, and a term $\underline{J}_A^{(p)}$ describing transport due to a pressure gradient. The ordinary diffusion component <u>defines</u> the molecular diffusion coefficient by Fick's law:

$$\underline{J}_A^{(m)} \equiv -CD\nabla x_A \tag{19}$$

where D is the binary diffusion coefficient in cm^2/sec and C is the total molar concentration of the mixture:

$$C = C_A + C_B \tag{20}$$

The mole fraction of species A is given by:

$$x_A = C_A/C \tag{21}$$

B. Elementary Kinetic Theory of Molecular Diffusion

Consider a binary mixture in which there exists a concentration gradient in the z-direction but no bulk fluid flow. As shown in Fig. 5, the net flux of A across a particular plane perpendicular to z may be regarded as the difference between the kinetic theory fluxes from regions a mean free path distant from the plane.

From kinetic theory, the rate at which molecules of A cross a unit area anywhere in the fluid is $1/4(n_A\bar{v}_A)$, where n_A is the molecular density of A and $\bar{v}_A$ is the mean speed of the molecules of A according to the Maxwell-Boltzmann distribution:

$$\bar{v}_A = \left(\frac{8kT}{\pi m_A}\right)^{1/2} \tag{22}$$

where k is the Boltzmann constant and m_A is the mass of a molecule of A. With respect to the above diagram, the molecular flux crossing the plane in the +z direction is:

$$\nu_A^+ = \frac{1}{4} N_{Av} \bar{v}_A \left(C_A - \frac{dC_A}{dz} \lambda\right)$$

where n_A has been written as Avogadro's number times the molar concentration. λ is the mean free path of

molecules of A in the mixture, given by:

$$\lambda = \frac{1}{\sqrt{2}\ \pi\sigma^2 n} = \frac{1}{\sqrt{2}\ \pi\sigma^2 N_{Av} C} \tag{23}$$

where σ is the diameter of the molecules (assumed the same for A and B, since only isotopic mixtures are considered here).

Similarly, the molecular flux in the -z direction is:

$$\nu_A^- = \frac{1}{4} N_{Av} \bar{v}_A \left(C_A + \frac{dC_A}{dz} \lambda \right)$$

The net molecular flux crossing the plane at z is the difference $\nu_A^+ - \nu_A^-$. Dividing this difference by avogadro's number to give the molar flux in the +z direction yields:

$$J_{Az}^{(m)} = \frac{\nu_A^+ - \nu_A^-}{N_{Av}} = -\frac{1}{2} \bar{v}_A \lambda \frac{dC_A}{dz}$$

Comparing this equation to the z-component of Eq. (19) for the present case (C=constant) shows that:

$$D = \frac{1}{2} \bar{v}_A \lambda$$

Using the kinetic theory expressions for $\bar{v}_A$ and λ yields:

$$CD = \left(\frac{kT}{\pi m_A} \right)^{3/2} \frac{1}{N_{Av} \pi \sigma^2} \tag{24}$$

Although derived by a very simplified model, Eq. (24) correctly predicts the ~3/2 power dependence of D upon absolute temperature, and the inverse variation of D with total concentration C. This latter characteristic is especially important in the gas centrifuge, where the total concentration (or pressure) varies by a factor of nearly 1000 across the radius.

C. Equilibrium Distribution in a Centrifugal Force Field

Consider the equilibrium situation shown in Fig. 6 of a fluid mixture spinning at angular velocity Ω rad/sec in a cylindrical tube of radius r_2. There is no bulk fluid motion and the temperature is everywhere T_o. The centrifugal force on a molecule of species A at radial distance r from the axis is:

$$F_r = \frac{m_A v_T^2}{r} = m_A r\Omega^2 \tag{25}$$

where v_T is the tangential velocity, $r\Omega$, at r. The potential energy of the particle relative to the position on the axis is the integral of the force:

$$E_p(r) = -\int_0^r F_r(r')dr' = -\frac{1}{2} m_A (r\Omega)^2 \tag{26}$$

Since the physical system is one of thermodynamic equilibrium at a constant temperature T_o, the ratio of the probability of finding a particle of A at a location r to the probability of finding one on the axis is given by the Boltzmann factor (20):

$$\exp[-E_p(r)/kT_o]$$

Or, since the probability of finding the particle at r is proportional to the concentration of A at r, the thermodynamic argument yields the equilibrium radial concentration profile.[4]

$$C_A(r) = C_A(0)\ \exp\left[\frac{M_A(r\Omega)^2}{2RT_o}\right] \tag{27}$$

where $M_A = N_{av} m_A$ is the molecular weight of species A and $R = N_{av} k$ is the gas constant. $C_A(0)$ is the concentration of A on the axis. Similarly, for species B:

$$C_B(r) = C_B(0)\exp\left[\frac{M_B(r\Omega)^2}{2RT_o}\right] \tag{28}$$

The sum of (27) and (28) gives the total concentration. Using (27), (28), in (20) and substituting in the definition of the mole fraction of Eq. (21) gives the radial concentration profile in mole fraction units:

$$x_A(r) = \left[1 + \left(\frac{1-x_A(0)}{x_A(0)}\right) e^{a^2 r^2}\right]^{-1} \tag{29}$$

where a^2 is:

$$a^2 = \frac{(M_B - M_A)\Omega^2}{2RT_o} \tag{30}$$

Because of the centrifugal force field, the light isotope (A) concentrates on the axis while the heavy isotope is enriched on the periphery. The equilibrium separation factor of the light isotope for a centrifuge of outer radius r_2 is given by:

$$\alpha_0 = \frac{x_A(0)/[1-x_A(0)]}{x_A(r_2)/[1-x_A(r_2)]}$$

Or, using Eq. (29) for $x_A(r_2)$:

$$\alpha_o = e^{a^2 r_2^2} \tag{31}$$

The equilibrium separation factor for uranium isotopes ($M_B - M_A = 3$) at a peripheral speed (Ωr_2) of 300 m/sec and 300°K is 1.055. Thus, the basic simple process difference, $\alpha_o - 1$, for the centrifuge is 0.055, which is more than an order of magnitude greater than the simple process difference for an ideal diffusion membrane, which is $\alpha_o - 1 = (M_B/M_A)^{1/2} - 1 = 0.0043$.

The equilibrium separation factor of Eq. (31) is not obtained in an actual centrifuge. The previous development applied to a situation in which there was no flow. In a real machine, there must be some internal flow at least to supply feed and remove waste and product. Some aspects of the internal flow tend to degrade the separation factor, but in the thermally driven countercurrent machine, the flow actually improves the enrichment by multiplying the simple process factor - the real centrifuge acts like a little cascade.

In order to describe the concentration distribution and enrichment in a real centrifuge, the species conservation equation, Eq. (18), must be applied to the device. To do this, we still need to provide a description of the pressure diffusion term, $\underline{J}_A^{(P)}$, to complete the definition of the flux $\underline{J}_A$. This is accomplished by considering the

equilibrium (no flow) case just discussed.

D. Pressure Diffusion Flux

The mole fraction profile established in the spinning fluid, Eq. (29), is a strictly thermodynamic relation and so does not depend upon the actual mechanism by which it was set up. However, we may regard it as a balance between the opposing mechanisms of ordinary molecular diffusion and pressure diffusion. In the equilibrium case, this balance takes the form:

$$J_{Az} = 0$$

$$J_{Ar} = J_{Ar}^{(m)} + J_{Ar}^{(p)} = 0 \tag{32}$$

where r and z refer to the radial and axial coordinates in the spinning fluid. Since $J_{Ar}^{(m)}$ is given by the r-component of Eq. (19):

$$J_{Ar}^{(m)} = -CD\left(\frac{dx_A}{dr}\right) \tag{33}$$

and $x_A(r)$ is given by Eq. (29), combination of Eqs. (29), (32), and (33) yields:

$$J_{Ar}^{(p)} = -CD(M_B - M_A)x_A(1-x_A)\frac{\Omega^2}{RT}r \tag{34}$$

Since there is no external force on the particles in the

z-direction,

$$J_{Az}^{(p)} = 0 \tag{35}$$

Even though Eq. (34) was derived for the case of an equilibrium situation, it is valid even when there is fluid motion[5], and Eqs. (34) and (35) provide the description of pressure diffusion needed to apply Eq. (18) to the gas centrifuge.

E. Fundamental Partial Differential Equation of the Countercurrent Gas Centrifuge

The vector fluid velocity, $\underline{v}$, in the centrifuge of Fig. 2 consists of radial, azimuthal and axial components u, v, and w. As will be shown in Sec. III, the radial component is zero, the aximuthal component is approximately equal to the solid body rotational speed $r\Omega$, and the axial component is a function of radial position alone. Axial fluid motion is generated inside the spinning rotor by two means:

(a) The top cover plate of the centrifuge is made somewhat hotter (by about 20°C) than the bottom plate. This temperature difference induces a natural ciruclation flow into the otherwise purely rotational motion of the gas. As shown by the arrows in the sketch, the flow is countercurrent in nature. The fluid moves downward near the axis and rises along the wall at the periphery. Except near the ends, this axial flow is a function of radial position

only, and is denoted by the function w(r). If axial distance is measured from the top end, w(r) is positive for radial locations near the axis and negative near the periphery. The magnitude of the axial circulation is controlled by the temperature difference between the end plates, and the shape to the profile is determined largely by the design of the rotor internals (e.g., the design of the scoops to remove product and waste and internal baffles, if any).

(b) The primary thermally-induced natural circulation flow described in (a) is perturbed by the introduction of feed gas on the axis and the withdrawal of waste and product from either end of the machine. It will be assumed that these external flows are but a small perturbation on the internal circulation.

Accepting the above restrictions on the velocity components, the convective term in Eq. (18) is:

$$\nabla\cdot(C_A\underline{v}) = \frac{\partial}{\partial z}(C_A w) = Cw\left(\frac{\partial x_A}{\partial z}\right) \tag{36}$$

The diffusive term in Eq. (18) is:

$$\nabla\cdot\underline{J}_A = \frac{1}{r}\frac{\partial}{\partial r}\left[r\left(J_{Av}^{(m)} + J_{Ar}^{(p)}\right)\right] + \frac{\partial J_{Az}^{(m)}}{\partial z} \tag{37}$$

the radial flux components are given by Eqs. (34) and (35) (with a partial derivative in the former):

$$J_{Ar} = J_{Ar}^{(m)} + J_{Ar}^{(p)} = -CD\left[\frac{\partial x_A}{\partial r} + 2a^2 x_A(1-x_A)r\right] \tag{38}$$

where a^2 is given by Eq. (30).

There is no pressure diffusion in the z-direction, and the component of the diffusion flux in this direction is due purely to molecular diffusion:

$$J_{Az} = J_{Az}^{(m)} = -CD \frac{\partial x_A}{\partial z} \tag{39}$$

Noting that by Eq. (24), the product CD is a constant, the steady state form of Eq. (18) for the centrifuge becomes:

$$Cw \frac{\partial x}{\partial z} = \frac{(CD)}{r} \frac{\partial}{\partial r} [r \frac{dx}{dr} + 2a^2 x(1-x)r^2] + (CD) \frac{\partial^2 x}{\partial z^2} \tag{40}$$

The subscript A on the mole fraction has been dropped for clarity of notation. C and w are functions of r only.

Eq. (40) is the fundamental equation whose solution gives the complete concentration field in a countercurrent gas centrifuge. No exact solution is obtainable, but a very good approximate solution can be obtained by noting that although C and w vary substantially with r, the variation of x with r is very small (less than in the equilibrium case, where x(r) is given by Eq. (29)). Because of the countercurrent flow established by the internal circulation, x varies more with z than with r. Therefore, we seek a solution for the radially-averaged mole fraction $\bar{x}(z)$ as a function of z.

F. Axial Enrichment Equations

We have alluded to the fact that the centrifuge acts like a small cascade, and analysis of the device must reflect this feature. The treatment here differs in this respect from that presented by Cohen (18), but is quite similar to the studies of Los (21) and Kanagawa and Oyama (22).

In Fig. 7, the centrifuge has been divided at the feed point into a stripping section and an enriching section. Just as in the analysis of a cascade, we take material balances on the desired isotope and on both isotopes in each section.

The net flux of the desired isotope across a cross section of the entire centrifuge in the enriching section ($z_F \leq z \leq Z$) must be equal to the rate at which this isotope leaves the device in the product, which is $x_p P$:

$$x_p P = 2\pi \int_{r_0}^{r_2} N_z(r) r dr \tag{41}$$

where N_z is the flux of the desired isotope in the $+z$ direction, given by a combination of Eqs. (17) and (19) for the particular restrictions of the centrifuge:

$$N_z = -CD \frac{\partial x}{\partial z} + xCw \tag{42}$$

Inserting (42) into (41), there results:

$$\frac{x_p P}{2\pi} = -(CD) \underbrace{\int_{r_0}^{r_2} r \frac{\partial x}{\partial z} dr}_{(B)} + \underbrace{\int_{r_0}^{r_2} Cwxrdr}_{(A)} \qquad (43)$$

The integral (A) is integrated by parts:

$$(A) = \int_{r_0}^{r_2} Cwxrdr = x(r_2) \int_{r_0}^{r_2} Cwrdr - \int_{r_0}^{r_2} \left(\frac{\partial x}{\partial r}\right) \int_{r_0}^{r} Cwr'dr' \, dr$$

We now define a <u>flow function</u>, f(r), by:

$$f(r) = \int_{r_0}^{r} Cwr'dr' \qquad (44)$$

so that the integral (A) is:

$$(A) = x(r_2)f(r_2) - \int_{r_0}^{r_2} f(r) \frac{\partial x}{\partial r} dr \qquad (45)$$

The radial concentration gradient in the last term of Eq. (45) must be estimated. It will always be smaller then the gradient in the equilibrium case, which from Eq. (29) is:

$$\left(\frac{dx}{dr}\right)_{eq} = -2a^2 x(1-x)r \qquad (46)$$

In the actual case, $\partial x/\partial r$ is obtained directly from the fundamental equation, Eq. (40), by carefully examining the

order of magnitude of the various terms. The variation of x with both r and z is small, but it is smaller in the r direction than in the z direction. If $\partial x/\partial z$ is small, then $\partial^2 x/\partial z^2$ is smaller still, and the last term in Eq. (40) may be neglected in the estimation of $\partial x/\partial r$. (Berman (23) has performed the analysis without this simplification). Similarly, the variation of $\partial x/\partial z$ with radial position is of slight importance compared to the variation of Cw with r in the left hand side of Eq. (40). Therefore, $\partial x/\partial z$ is approximated by $d\bar{x}/dz$, which by definition, is independent of r. Thus, <u>for the purpose of estimating $\partial x/\partial r$</u>, Eq. (40) becomes:

$$Cw \frac{d\bar{x}}{dz} = \frac{(CD)}{r} \frac{\partial}{\partial r} \left[r \frac{\partial x}{\partial r} + 2a^2 \bar{x}(1-\bar{x}) r^2 \right] \tag{47}$$

In a similar spirit, the mole fractions appearing in the last term of Eq. (47) have been taken as the radially averaged values. Eq. (47) is multiplied by rdr and integrated from r_0 to r. At $r=r_0$, the bracketed quantity in Eq. (47), which is proportional to the radial flux, is zero. Solving for the radial gradient:

$$\frac{\partial x}{\partial r} = -2a^2 \bar{x}(1-\bar{x}) r + \frac{1}{(CD)} \frac{f(r)}{r} \left(\frac{d\bar{x}}{dz} \right) \tag{48}$$

The flow function of Eq. (44) has been used to obtain Eq. (48). The first term on the right of Eq. (48) is the equilibrium radial concentration gradient, given by Eq. (46)

The last term represents a degradation of the gradient due to the internal flow in the device.

Eq. (48) is now substituted into Eq. (45) to give:

$$\textcircled{A} = \bar{x}f(r_2) + 2a^2\bar{x}(1-\bar{x})\int_{r_0}^{r_2} rf(r)dr - \frac{1}{(CD)}\left(\frac{d\bar{x}}{dz}\right)\cdot$$

$$\int_{r_0}^{r_2} \frac{f^2(r)}{r}\,dr \qquad (49)$$

where $x(r_2)$ in Eq. (45) has been approximated by the average concentration, $\bar{x}$.

In the Ⓑ integral of Eq. (43), $\partial x/\partial z$ is approximated by $d\bar{x}/dz$ and removed from the integral:

$$\textcircled{B} = \frac{1}{2}\,r_2^2\,\frac{d\bar{x}}{dz} \qquad (50)$$

Using Eqs. (49) and (50) for the Ⓐ and Ⓑ integrals, Eq. (43) becomes:

$$\bar{x}f(r_2) + \left[2a^2\int_{r_0}^{r_2} rf(r)dr\right]\bar{x}(1-\bar{x}) - \frac{1}{(CD)}\cdot$$

$$\left[\int_{r_0}^{r_2} \frac{f^2(r)}{r}\,dr\right]\frac{d\bar{x}}{dz} = \frac{1}{2}(CD)r_2^2\,\frac{d\bar{x}}{dz} + \frac{x_P P}{2\pi} \qquad (51)$$

which is an ordinary differential equation describing the variation of the radially-averaged mole fraction, $\bar{x}$, with

axial position z. It may be written in a more compact form by collecting the bracketed coefficients as constants and omitting the bar over x:

$$\frac{1}{g}\frac{dx}{d\eta} = x(1-x) - \gamma P(x_p - x) \tag{52}$$

where:

$$\eta = z/Z \tag{53}$$

and

$$\frac{1}{\gamma} = 2a^2 r_2^2 \int_{\sigma}^{1} F(\zeta)\zeta d\zeta \tag{54}$$

$$\frac{1}{\gamma g} = \left\{ \frac{1}{2}(2\pi C D r_2) + \frac{\int_{\sigma}^{1} [F(\zeta)]^2 \frac{d\zeta}{\zeta}}{(2\pi C D r_2)} \right\} \frac{1}{(Z/r_2)} \tag{55}$$

the flow function integrals in (56) and (55) have been written in terms of the dimensionless radial position

$$\zeta = r/r_2 \tag{56}$$

and σ is r_0/r_2.

In terms of ζ (and multiplied by 2π), the flow function is:

$$F(\zeta) = 2\pi r_2^2 \int_{\sigma}^{\zeta} C w \zeta' d\zeta' \tag{57}$$

The total product flow rate, P, is related to the

flow function by the following argument. Material balances formulated for the other isotope are similar to Eqs. (41) and (42) except that x_p is replaced by $1-x_p$ and x by 1-x. Adding the equations for the two isotopes yields:

$$P = 2\pi \int_{r_0}^{r_2} Cwrdr$$

or, in terms of the flow function:

$$P = F(1) \tag{58}$$

Eq. (58) was used in transforming Eq. (51) to Eq. (52).

Eq. (52) is the basic radially-averaged differential equation for the concentration variation in the enriching section of the centrifuge ($z_F \leqq z \leqq Z$, or $\eta_F \leqq \eta \leqq 1$). In the stripping section ($0 \leqq \eta \leqq \eta_F$), a similar derivation produces the equation:

$$\frac{1}{g^*} \frac{dx}{d\eta} = x(1-x) - \gamma^* W(x-x_W) \tag{59}$$

where x_W and W are the waste composition and flow rate, respectively. The coefficients g* and γ^* are of the same form as Eqs. (54) and (55) except that the flow function therein is based upon the axial velocity profile in the stripping section:

$$F^*(\zeta) = 2\pi r_2^2 \int_{\sigma}^{\zeta} Cw^* \zeta' d\zeta' \tag{60}$$

The waste flow rate is given by:

$$W = -F^*(1) \tag{61}$$

The flow function $F^*(\zeta)$, and hence the coefficients g^* and γ^*, differ from the analagous parameters in the enriching section because of the difference in the axial velocity w(r) in the two sections. These two are slightly different for the reasons described in (b) of Sec. IIE.

If there were no feed or withdrawal from the centrifuge (i.e., total reflux), a flow profile $w_{TR}(r)$ would be established by the temperature difference between the cover plates. As shown in Fig. 2, the feed is introduced on the axis somewhere in between the ends of the centrifuge. The feed joins the downward flow in the core. Part of the flow added at the feed point is removed at the product end, but the rest remains with the circulatory flow and moves upward toward the waste end. The last vestige of feed gas is removed at the top and the main circulating flow moves down to the feed point to again pick up feed. The perturbation of the axial velocity profile and the flow function due to the feed are shown in Fig. 8. (w is zero at $r=r_0$ and r_2 because of the solid boundaries, where we have assumed the "no slip" condition to apply.)

As suggested by Fig. 8, we assume that the perturbation in the total reflux profile, $w_{tr}(r)$ is slight. It cannot be vanishingly small, however, for the flow function of Eq. (57) at $\zeta=1$ must be equal to P in the enriching section

(Eq. (58)) and -W in the stripping section. However, except at $\zeta=1$, we do not need to carry the distinction betweem w_{TR} and w or w_{TR} and w*. In particular the flow function $F(\zeta)$ in Eqs. (54) and (55) can be adequately calculated from <u>any</u> of the velocity profiles in the sketch without altering the values of the integrals appreciably. The net effect of this approximation is that the coefficients g and γ in the enriching section are the same as the coefficients g* and γ* in the stripping section, or the asterisks in Eq. (59) may be omitted.

The approximation just discussed is valid provided that the external flow rates P and W are small compared to the <u>magnitude</u> of the internal flow. The magnitude of the internal flow is measured by the integral of the axial velocity profile <u>without regard to the sign of w(r)</u>, or a flow rate M is defined by:

$$M = 2\pi r_2^2 \int_{\sigma}^{1} C|w|\zeta d\zeta \qquad (62)$$

which is the sum of the concentration-weighted areas of the positive and negative portion of the w(r) curve of Fig. 8.

M is controlled solely by the temperature difference between the cover plates. If L is the throughput (feed) of the centrifuge, then the requirement that the external flow exert a negligible influence on the thermal circulation is equivalent to requiring that the <u>reflux ratio</u>, L/M, be much smaller than unity. Berman (23) and Ouwerkerk and Los (24) have included the effect of non-negligible

feed rate in the centrifuge calculations. The net effect is a reduction in separative power.

The internal flow rate M has another useful application. It serves as a scale factor for the integrals in Eqs. (54) and (55). The flow pattern <u>efficiency</u> is defined by:

$$E = \frac{4\left\{\int_{\sigma}^{1} F(\zeta)\zeta d\zeta\right\}^2}{\int_{\sigma}^{1} [F(\zeta)]^2 \frac{d\zeta}{\zeta}} \tag{63}$$

and a flow number is defined by:

$$N_f = \frac{M}{4\left\{\int_{\sigma}^{1} [F(\zeta)]^2 \frac{d\zeta}{\zeta}\right\}^{1/2}} \tag{64}$$

Because of the scaling by the internal flow magnitude, M, the factors E and N_f are independent of both the throughput L and the internal flow magnitude, M. In terms of these factors, the coefficients g and γ of Eqs. (54) and (55) may be written as:

$$\frac{1}{\gamma} = \left(\frac{a^2 r_2^2 \sqrt{E}}{4N_f}\right) M \tag{65}$$

$$g = \frac{\left(\frac{a^2 r_2^2 \sqrt{E}}{4N_f}\right)\left(\frac{Z}{r_2}\right) M}{\frac{1}{2}[2\pi C D r_2] + \frac{1}{16}\left[\frac{1}{2\pi C D r_2}\right]\frac{M^2}{N_f^2}} \tag{66}$$

G. Enrichment at Total Reflux

When there is no feed added to or waste and product withdrawn from the centrifuge, the last terms in Eqs. (52) and (59) vanish. If, in addition, we confine attention to the case of low enrichment, $x \ll 1$ (which merely simplifies the mathematics but does not affect the main features of the final results), the enrichment equations for both sections are identical and may be written as:

$$\frac{dx}{d\eta} = gx \tag{67}$$

which is valid from $\eta=0$ to $\eta=1$. Integration of (67) over these limits yields:

$$\frac{x_P}{x_F} = e^g \tag{68}$$

Now, the separation factor of any separating unit is defined by the ratio of the product and waste abundance ratios according to Eq. (3). In the case of $x \ll 1$ considered here, $\alpha = x_P/x_W$, so that Eq. (68) is the separation factor at total reflux:

$$\alpha_{TR} = e^g \tag{69}$$

Since the ratio g is a function only of the internal flow rate M (by Eq. (66), α_{TR} varies with M in the manner sketched in Fig. 9.

As $M \to 0$, $g \to 0$ and the left hand term in the denominator

of Eq. (66) is dominant. This term, if it is followed back through the derivation, represents axial molecular diffusion. The limit $\alpha_{TR} \to 1$ as $M \to 0$ simply states that if no internal circulation is established, no axial enrichment can be attained. At small M, axial enrichment is severaly restricted by back diffusion in the z direction.

Similarly, $g \to 0$ as $M \to \infty$ and the right hand term in the denominator

of Eq. (66) is much larger than the axial diffusion term. In this limit, the axial enrichment is reduced by the very large circulation currents which are implied by large M. In the limit, the strong circulatory flow simply uniformly mixes up the entire contents of the centrifuge.

The maximum enrichment at total reflux occurs at an internal flow rate given by:

$$M_0 = 2\sqrt{2}(2\pi CDr_2)N_f \tag{70}$$

(this optimum M is obtained by setting $\frac{dg}{dM} = 0$).

When $M=M_o$, Eqs. (66) and (69) give:

$$\alpha_{TR,opt} = \exp\left[\frac{1}{\sqrt{2}}(a^2 r_2^2)\sqrt{E}\left(\frac{Z}{r_2}\right)\right] \tag{71}$$

This is a very instructive equation. Compare it to the equilibrium separation factor of Eq. (31). Whereas the equilibrium case represents an enrichment in the radial direction ($r=0$ compared to $r=r_2$), Eq. (71) is an enrichment factor for the axial direction ($z=0$ compared to $z=Z$). By the establishment of the internal circulation, the direction of largest enrichment has been changed from radial to axial. Naturally, in an actual centrifuge, the product and waste are withdrawn from the ends of the machine rather than from the axis and periphery. Moreover, the axial enrichment is larger than the equilibrium enrichment.

The term $a^2 r_2^2$ in the exponent of Eq. (71) is the equilibrium separation difference, $\alpha_o - 1$. The flow pattern efficiency term ($\sqrt{E}$) represents a degradation of enrichment due to the flow in the device - it must have a value less than unity. The last term, the length-to-radius ratio, represents the augmentation of the enrichment due to the countercurrent flow in the centrifuge.

If the following values are assumed (all are typical of actual centrifuges):

$$a^2 r_2^2 = 0.055$$

$$E = 0.7$$

$$Z/r_2 = 7$$

we obtain $\alpha_{TR,opt} = 1.25$, which represents a simple process difference ∿50 times greater than can be achieved in the gaseous diffusion process. However, this very large enrichment has only been obtained with no throughput, which is obviously not a practical way of operating an isotope separating unit. We must now investigate how a non-zero throughput reduces the separation factor, and develop a means of optimizing the performance of the centrifuge.

H. Effect of Throughput on Enrichment

The enrichment attainable by a centrifuge when the external flows L, P, and W are not zero is governed by Eqs. (52) and (59) (with the primes removed in the latter

relation). For the low concentration case ($x<<1$), these equations can be integrated to yield:

$$\frac{x_P}{x} = \frac{(1+\gamma P)\exp[g(1+\gamma P)(1-\eta)]}{1 + \gamma P\exp[g(1+\gamma P)(1-\eta)]} \tag{72}$$

for $\eta_F \leq \eta \leq 1$ (enriching section), and:

$$\frac{x}{x_W} = \frac{\exp[g(1-\gamma W)\eta]-\gamma W}{1-\gamma W} \tag{73}$$

for $0 \leq \eta \leq \eta_F$ (stripping section).

It is convenient to express the total internal flow rate, M, in terms of its optimum value at total reflux by the ratio:

$$m = M/M_o \tag{74}$$

where M_o is given by Eq. (70).

In terms of the reduced internal flow parameter, the coefficients g and γ become:

$$\frac{1}{\gamma} = \frac{1}{\sqrt{2}} (a^2 r_2^2)\sqrt{E}[2\pi C D r_2]m \tag{75}$$

$$g = \frac{1}{\sqrt{2}} (a^2 r_2^2)\sqrt{E}\left(\frac{Z}{r_2}\right)\left(\frac{2m}{1+m^2}\right) \tag{76}$$

Both γ and g are functions of the experimentally controllable internal flow rate via the parameter m, but are independent of the throughput, which appears in Eqs. (72) and (73) as the quantities P and W.

We now join the enricher and stripper equations ((72) and (73)) at the feed point by inserting $x=x_F$ at $\eta=\eta_F$ in both relations. In order to avoid mixing of fluids of different composition, the feed is introduced at the axial location where the common concentration in the stripper and enricher at the feed point is equal to the feed concentration. Instead of expressing the external flows as P and W, it is more convenient to use the throughput (or feed rate) L and the cut θ. The ratio x_P/x_F which appears on the left of Eq. (72) at $\eta=\eta_F$, may be rewritten by use of Eqs. (2) and (3)

$$\frac{x_P}{x_F} = \frac{x_P}{x_P\theta + x_W(1-\theta)} = \frac{\alpha}{1 + (\alpha-1)\theta} \tag{77}$$

The second equality is a result of identifying x_P/x_W with the separation factor α. In terms of the cut, γP may be written as $\theta\gamma L$, so that at the feed point, Eq. (72) becomes:

$$\frac{\alpha}{1 + (\alpha-1)\theta} = \frac{(1+\theta\gamma L)\exp\{g(1-\eta_F)(1+\theta\gamma L)\}}{1 + (\theta\gamma L)\exp\{g(1-\eta_F)(1+\theta\gamma L)\}} \tag{78}$$

Similarly, Eq. (73) is:

$$1 + (\alpha-1)\theta = \frac{\exp\{g\eta_F[1-(1-\theta)\gamma L]\} - (1-\theta)\gamma L}{1 - (1-\theta)\gamma L} \tag{79}$$

In principal, the parameter η_F can be eliminated between

Eqs. (78) and (79), and these two equations may be regarded as a single relation providing the separation factor α as a function of the parameters θ, γL, and g. Once the centrifuge is designed and the rotational speed and the gaseous feed specified (i.e., UF_6), the following parameters are fixed:

$a^2 r_2^2$ = equilibrium separation difference

E = flow pattern efficiency

Z/r_2 = geometric factor

$[2\pi CDr_2]$ = molecular diffusion factor

The first three of these factors are dimensionless. The diffusion factor has the units of flow rate, and may be expressed in moles/sec or kg/yr.

Hence, g and γ are functions only of the internal flow parameter m and Eqs. (78) and (79) are equivalent to the relation $\alpha(\theta, L, m)$. These three independent variables are controllable parameters of the centrifuge. θ and L are controlled by valves on the external flow lines and m is adjusted by the temperature difference between the end plates of the machine.

The behavior of α with m for the limiting case L=0 was described in section IIG. In the general case, for a fixed cut, the variation of α with m exhibits a maximum for each value of L, as sketched in Fig. 10.

The optimum value of m is unity at L=0, but moves to larger m as L is increased. The maxima in the above curves describe α_{opt} as a function of L, which are plotted in Fig. 11.

I. Close-Separation Approximation for α in the Case of Non-Zero Throughput

The graphs in the preceding section show that as L increases, the maximum attainable separation factor α decreases and occurs at increasingly larger values of m. A practical centrifuge is operated in a region where m is significantly greater than unity (i.e., 2 or 3) so that

$$\frac{2m}{1+m^2} < 1$$

The product of the remaining factors in Eq. (76) are also less than unity (in the example in Sec. IIG, this product was 0.23), so that we can seek a solution of Eqs. (78) and (79) in the limit as

$$g \to 0 \qquad (80)$$

However, if this limit is directly applied to Eqs. (78) and (79), only the trivial solution α=1 results. Therefore, we must also require that:

$$g\gamma L \text{ is not vanishingly small} \qquad (81)$$

even though g is very small. This combination is satisfied if

$$\gamma L \text{ is large} \qquad (82)$$

Since throughput rates greater than zero reduce α below its value at total reflux, the close separation approximation can be applied to the left hand side of Eq. (78), which becomes:

$$\frac{\alpha}{1+(\alpha-1)\theta} \simeq \alpha[1-(\alpha-1)\theta] = [1+(\alpha-1)][1-(\alpha-1)\theta] \simeq$$

$$1 + (\alpha-1)(1-\theta) \tag{83}$$

Applying conditions (80) and (82) to the right hand side of Eq. (78), we obtain:

$$\frac{\left(1 + \frac{1}{\theta\gamma L}\right) \exp[g(1-\eta_F)\theta\gamma L]}{\frac{1}{\theta\gamma L} + \exp[g(1-\eta_F)\theta\gamma L]} \simeq 1 + \frac{1 - \exp[-g(1-\eta_F)\theta\gamma L]}{\theta\gamma L} \tag{84}$$

the right hand side of (84) follows by assuming $\theta\gamma L >> 1$.

Equating (83) and (84) yields:

$$(\alpha-1)(1-\theta) = \frac{1 - \exp[-g(1-\eta_F)\theta\gamma L]}{\theta\gamma L} \tag{85}$$

Applying identical arguments to Eq. (79) produces:

$$(\alpha-1)\theta = \frac{1 - \exp[-g\eta_F(1-\theta)\gamma L]}{(1-\theta)\gamma L} \tag{86}$$

Examination of these two equations shows that for both to be valid, the arguments in the exponential terms must be equal; this can occur only if

$$\eta_F = \theta \tag{87}$$

which, if used in either (85) or (86) results in:

$$\alpha-1 = g\left\{\frac{1 - \exp[-g\gamma(1-\theta)\theta L]}{[g\gamma(1-\theta)\theta L]}\right\} \tag{88}$$

Eq. (88) gives a quite satisfactory description of the enrichment capability of a centrifuge under the conditions $m>1$, $L>0$, $\alpha-1$ small. Eq. (87) also shows that the point at which the feed is introduced into the machine is specified by the desired cut.

J. Optimum Separative Power of a Centrifuge

It has been indicated in rather loose terms that centrifuges are usually operated with relatively large values of m, with L of course greater than zero, and with a simple process difference appreciably smaller than obtainable at total reflux. In this section, these conditions are made quantitative. The main question which arises is what criteria should be applied to select optimum values of m, L, and θ. This question is answered by the considerations of Sec. ID.

According to Eq. (15), the number of separating units in a cascade of specified total separative capacity U is minimized if the separative power of each unit is maximized. Consequently, we determine values of L, m and θ which maximize δU. This optimization procedure is different from that discussed in Sec. IIH. In the latter,

θ and L were fixed and m was chosen to maximize α. In the present case, we shall fix m and choose θ and L to maximize δU. Optimization of the controllable variables to give the largest separative power is more important than adjustments to achieve the largest separation factor; δU determines the number of centrifuges required in a cascade, whereas α merely determines how the fixed number of units is to be arranged in the ideal cascade.

With the restriction of close separation (which has already been incorporated into the analysis of α), the separative power of any separating unit is given by Eq. (11). If Eq. (88) is inserted into Eq. (11), there results:

$$\delta U = \frac{1}{2}\left|\frac{g}{\gamma}\right| \frac{\{1 - \exp[-g\gamma(1-\theta)\theta L]\}^2}{[g\gamma(1-\theta)\theta L]} \tag{89}$$

In the limiting case of close separation, both α and δU depend only upon two controllable parameters - the product θ(1-θ)L and m (which governs g and γ). If we regard m (and hence g and γ) as fixed, the maximum separative power occurs when the right hand side of Eq. (89) is a maximum, or when:

$$[g\gamma(1-\theta)\theta L]_{opt} = 1.25643\,1208\cdots \tag{90}$$

at which point:

$$\delta U_{opt} = \frac{1}{2}(0.41)\left|\frac{g}{\gamma}\right| \tag{91}$$

$$\downarrow$$

$$.4072643776\cdots$$

Inserting the expressions for g and γ from Eqs. (75) and (76) into Eq. (91):

$$\delta U_{opt} = 0.81E\left\{\frac{1}{4}(a^2 r_2^2)^2 (2\pi C D r_2)\left(\frac{Z}{r_2}\right)\right\}\left(\frac{m^2}{1+m^2}\right) \qquad (92)$$

The quantity in the curly brackets of Eq. (92) is shown in the Appendix to be the maximum possible separative power of any type of centrifuge, δU_{max}. It is thus a standard against which the performance of the thermally driven countercurrent variety can be compared.

The overall efficiency is defined by:

$$\text{overall efficiency} = \frac{\delta U_{opt}}{\delta U_{max}} = 0.81E\left(\frac{m^2}{1+m^2}\right) \qquad (93)$$

The overall efficiency contains three terms, each of which is less than unity.

The constant 81% efficiency contribution in Eq. (93) stems from the nature of the thermally driven countercurrent in the centrifuge considered here. Los (21,24) has shown that this loss of separative power is due to the fact that the direction of fluid flow changes from axial in the middle of the bowl to radial at the ends of the centrifuge, where the internal flow changes direction by 180°. The net effect is a reduction in the effective length of the bowl. This factor is not present in the externally driven centrifuge of Fig. 1, where the flow is in the axial direction throughout the entire unit.

The second factor in Eq. (93), E, represents a degradation of efficiency due to the deviation of the pattern of the axial velocity profile from the optimum shape. This factor will be considered in more detail in Sec. III.

The last factor in Eq. (93) reflects the effect of the magnitude of the internal flow upon separative performance.

The separation factor under conditions that produce the maximum separative power is obtained from Eqs. (88) and (90):

$$\alpha_{opt} - 1 = g\frac{1 - e^{-1.25}}{1.25} = 0.57g$$

or

$$\alpha_{opt} - 1 = \frac{1}{2}(0.81)(a^2 r_2^2)\sqrt{E}\left(\frac{Z}{r_2}\right)\left(\frac{2m}{1+m^2}\right) \tag{94}$$

Similarly, the optimum throughput is obtained from Eq. (90) as:

$$L_{opt} = \frac{0.63(2\pi CDr_2)}{(1-\theta)\theta(Z/r_2)}(1+m^2) \tag{95}$$

The value of the internal flow parameter which maximizes the separative power is seen from Eq. (92) to be $m=\infty$. Obviously, this is a practically unattainable limit, since the separation factor would be unity by Eq. (94) and the throughput rate would be infinite according to

Eq. (95). A practical compromise is to operate in the neighborhood of m=3, at which point,

$$\frac{m^2}{1+m^2} = 0.9$$

and

$$\frac{2m}{1+m^2} = 0.6$$

At m=3, the separative power is 90% of the maximum value, yet the enrichment per stage is still 60% of its maximum.

It will be recalled from the discussion of Sec. IIF that one of the requirements of the analysis was that the reflux ratio, L/M, be much less than unity. This restriction ensured that the throughput did not appreciably alter the internal flow established by the natural convection process. If this is not true, the overall efficiency is smaller than that given by Eq. (93), wherein the first factor is less than 0.81 (24). The reflux ratio under optimum conditions is obtained from Eq. (92) with the use of Eq. (70):

$$\left(\frac{L_{opt}}{M}\right) = \left(\frac{L_{opt}}{M_o}\right)\frac{1}{m} = \frac{1.25}{2\sqrt{2}(1-\theta)\theta(Z/r_2)N_f}\left(\frac{1+m^2}{2m}\right) \qquad (96)$$

In order to minimize the reflux ratio at the optimum separative power, the centrifuge should be long (large Z/r_2) and the cut should be $\frac{1}{2}$ (which maximizes $\theta(1-\theta)$). Since the cut enters only in the reflux ratio (and not

in δU_{opt} or α_{opt}), minimization of the reflux ratio is the only criterion for fixing the cut at $\frac{1}{2}$. This statement is valid only in the close separation limit, where the approximations used in Sec. II-I result in combining the variables θ and L into the single parameter $\theta(1-\theta)L$. Bulang et at (25) have shown that the optimum cut is less than $\frac{1}{2}$ in the general case.

K. Summary

A summary of the assumptions contained in the preceding analysis is given below:

(a) $x \ll 1$ (i.e., $x \lesssim 0.03$)

(b) α-1 small (i.e., <0.1)

(c) m large in order to satisfy conditions (84)-(82); (m=3 is large enough)

(d) reflux ratio $\ll 1$

(e) the feed is introduced at the position where the concentration of the feed point is equal to the feed composition.

Assumptions (a)-(c) have been introduced solely for calculational convenience and can readily be removed. Analyses similar to that presented here but without assumption (d) have been reported by Ouwerkerk and Los (24) and Berman (23). Point (e) is more of a specification than an

assumption; it should never be relaxed.

Typical parameters of a gas centrifuge utilizing uranium hexafloride as a process gas are shown in Table 1.

TABLE 1

TYPICAL PARAMETERS OF A GAS CENTRIFUGE (UF_6)

Peripheral velocity, Ωr_2 = 300m/sec

Z = 66cm[a]

r_2 = 9.3cm[a]

$a^2 r_2^2$ = 0.055

E = 0.7

CD = 2.2×10^{-4} gm/cm-sec @ 300°K[b]

$2\pi CDr_2$ = 400kg UF_6/yr

m=3 (assumed)

$\theta = \frac{1}{2}$

g=0.14

$1/\gamma$ = 40kg/yr

δU_{max} = 2.1kg/yr

Overall Efficiency = (0.81)(0.7)(0.9) = 0.51

δU_{opt} = 1.1kg/yr

L_{opt} = 1400kg/yr

α_{opt} = 1.08

[a] Ref. 9

[b] Ref. 23

III. HYDRODYNAMICS

A. Features of the Flow Needed for the Separative Analysis

The performance of a thermally driven countercurrent centrifuge which has been optimized for maximum separative power is governed by Eqs. (92), (94), and (95). All parameters in these equations are known except those which depend upon the axial velocity profile.

The dimensionless internal flow parameter, m, depends upon both the shape and magnitude of the internal flow, m is given by combination of Eqs. (74), (70), and (64) as[6]:

$$m = \frac{\left\{2\int_{\sigma}^{1} [F(\zeta)]^2 \frac{d\zeta}{\zeta}\right\}^{1/2}}{(2\pi\rho D r_2)} \tag{97}$$

The flow pattern efficiency, E of Eq. (63), depends only upon the shape of the flow function, but not upon its magnitude:

$$E = \frac{4\left\{\int_{\sigma}^{1} F(\zeta)\zeta d\zeta\right\}^2}{\int_{\sigma}^{1} [F(\zeta)]^2 \frac{d\zeta}{\zeta}} \tag{63}$$

where $F(\zeta)$ is given by Eq. (57). The flow function is subject to the restraint:

$$F(\sigma) = 0 \tag{98}$$

Throughout this review, we have assumed that the internal

circulation established by natural convection is but negligibly perturbed by the introduction of feed and withdrawal of product and waste. If so, the properties of the internal flow are those at total reflux, which supplies another restraint on the flow function:

$$F(1) = 0 \tag{99}$$

There are two levels of understanding required of the hydrodynamics in the centrifuge: knowledge of the axial velocity to within an undetermined multiplicative constant is sufficient to fix E; if in addition, the internal circulation parameter m is desired, the multiplicative factor must be determined.

B. The Optimal Flow Function

The optimal flow function is the one which produces a flow pattern efficiency, E, of unity. It can be deduced without considering the fluid mechanics of the centrifuge.

(1) Mathematical Approach

We first transform Eq. (63) by introducing the quantity:

$$F^*(\zeta) = F(\zeta)/\zeta^2 \tag{100}$$

and changing the radial variable to:

$$X = \zeta^4 \tag{101}$$

Using Eqs. (100) and (101) in Eq. (63) yields:

$$E = \frac{\left[\int_0^1 F^*(X)\,dX\right]^2}{\int_0^1 [F^*(X)]^2\,dX} \tag{102}$$

We have also assumed that $\sigma^4 << 1$, so that the lower limit on the integrals is replaced by zero.

The Schwarz inequality (26) states that for two functions f(X) and g(X) defined over the interval $0 \leq X \leq 1$,

$$\left[\int_0^1 f(X)g(X)\,dX\right]^2 \leq \left[\int_0^1 [f(x)]^2\,dX\right]\left[\int_0^1 [g(x)]^2\,dX\right] \tag{103}$$

where the equality holds only if f and g are proportional. If we take f(X) = F*(X) and g(X) = constant, Eq. (103) becomes:

$$\left[\int_0^1 F^*(X)\,dX\right]^2 \leq \int_0^1 [F^*(X)]^2\,dX \tag{104}$$

and the equality holds only if F*(X) is also a constant (since it must be proportional to g(X) which is a constant). Applying Eq. (104) to Eq. (102) shows that E must always be less than or equal to unity, the equality occuring only if F*(X) is a constant. If this is true, Eq. (100) requires that:

$$F_{opt}(\zeta) = \text{constant} \times \zeta^2, \qquad \text{for } E=1 \tag{105}$$

(2) Physical Approach

Los and Kistemaker (27) and Bock (28) have derived the optimal flow function by the following physical argument. The optimal velocity profile is the one which maximizes the separative power of the centrifuge. In the Appendix, it is shown that maximum separative power is attained when the radial concentration gradient, $\partial x/\partial r$, is one half of the equilibrium value (see Eq. (A-20)). The actual radial concentration profile in the centrifuge is given by Eq. (48). If Eq. (A-19) is inserted into the left hand side of Eq. (48), we see that under optimal conditions, $f(r) \sim r^2$, which is equivalent to Eq. (105).

(3) Implications of the Optimal Flow Function

In terms of the definition of the flow function by Eq. (57), Eq. (105) is obtained only if:

$$\rho w = \text{constant} \tag{106}$$

For a single component gas of molecular weight M, Eq. (27) shows that the total concentration varies with radial position according to:

$$\rho(\zeta) = \rho(0)e^{A^2\zeta^2} \tag{107}$$

where:

$$A^2 = \frac{M\omega^2 r_2^2}{2RT_o} = \left[\frac{(\omega r_2)}{\left(\frac{2RT_o}{M}\right)^{1/2}}\right]^2 \tag{108}$$

is the analog of the group $(a^2 r_2^2)$ used in the separative analysis. The second equality in Eq. (108) shows that A is the ratio of the peripheral speed to the most probable molecular speed of the Maxwell-Boltzmann distribution.

Combining Eqs. (108) and (107) shows that the optimal velocity profile is:

$$w_{opt}(\zeta) = \text{constant} \times e^{-A^2\zeta^2} \tag{109}$$

This axial velocity profile is unattainable in practice because it is of the same sign at all radial positions. As sketched in Fig. 8, the axial velocity must change sign at some point within the centrifuge, because of the counter-current nature of the flow. Violation of this physical requirement is equivalent to the fact that the optimal flow function of Eq. (105) does not satisfy the restraint of Eq. (99), imposed by the condition of total reflux.

Eq. (109) shows the type of velocity profile most advantageous to the separative performance of a gas centrifuge. In the remainder of this section, the actual hydrodynamics of the centrifuge are analyzed in order to determine how closely the optimal flow pattern can be approached. In addition, theoretical studies which seek to determine the magnitude of the internal flow are also reviewed.

C. Equations of Motion

(1) General Form

The complete velocity field inside the spinning

rotor of the gas centrifuge (assuming the fluid to be a single component ideal gas) is determined by the equations of motion. These are shown in full on pp. 83, 85, and 319 of Ref. 19. In cylindrical coordinates with axial symmetry and at steady state, they are:

overall mass continuity:

$$\frac{1}{r}\frac{\partial}{\partial r}(\rho r V_r) + \frac{\partial}{\partial z}(\rho V_z) = 0 \tag{110}$$

radial momentum:

$$\rho\left(V_r\frac{\partial V_r}{\partial r} - \frac{V_\theta^2}{r} + V_z\frac{\partial V_r}{\partial z}\right) = -\frac{\partial p}{\partial r} + \mu\left\{\frac{\partial}{\partial r}\left[\frac{1}{r}\frac{\partial}{\partial r}(rV_r)\right] + \frac{\partial^2 V_r}{\partial z^2}\right\} \tag{111}$$

angular momentum:

$$\rho\left(V_r\frac{\partial V_\theta}{\partial r} + \frac{V_r V_\theta}{r} + V_z\frac{\partial V_\theta}{\partial z}\right) = \mu\left\{\frac{\partial}{\partial r}\left[\frac{1}{r}\frac{\partial}{\partial r}\left(rV_\theta\right)\right] + \frac{\partial^2 V_\theta}{\partial z^2}\right\} \tag{112}$$

axial momentum:

$$\rho\left(V_r\frac{\partial V_z}{\partial r} + V_z\frac{\partial V_z}{\partial z}\right) = -\frac{\partial p}{\partial z} + \mu\left\{\frac{1}{r}\frac{\partial}{\partial r}\left(r\frac{\partial V_z}{\partial r}\right) + \frac{\partial^2 V_z}{\partial z^2}\right\} + \rho g \tag{113}$$

where V_r, V_θ, and V_z are the components of the fluid velocity in the radial, azimuthal, and axial directions. ρ and μ are the mass density and viscosity of the gas respectively, and g is the acceleration of gravity (assumed to be in the +z direction). The gas pressure is denoted by p. The term V_θ^2/r in the radial momentum equation and the term $V_r V_\theta/r$ in Eq. (112) represent the centrifugal and Coriolis forces, respectively. These forces arise solely from the spinning motion of the fluid and are absent in the momentum equations in rectangular coordinates.

The energy equation is:

$$\rho C_V\left(V_r \frac{\partial T}{\partial r} + V_z \frac{\partial T}{\partial z}\right) + T\left(\frac{\partial p}{\partial T}\right)_\rho\left[\frac{1}{r}\frac{\partial}{\partial r}(rV_r) + \frac{\partial V_z}{\partial z}\right] = \kappa\left[\frac{1}{r}\frac{\partial}{\partial r}\left(r\frac{\partial T}{\partial r}\right) + \frac{\partial^2 T}{\partial z^2}\right] \tag{114}$$

where C_v and κ are the specific heat at constant volume and the thermal conductivity of the gas, respectively. The second term on the left hand side of Eq. (114) represents the reversible work done on the fluid due to compression or expansion. Viscous dissipation has been neglected.

The equation of state of the ideal gas is

$$pM = \rho RT \tag{115}$$

where R is the gas constant and M is the molecular weight.

(2) The Equilibrium Solution

In the equilibrium case considered in Sec. IIC, there is no internal circulation and the velocity components reduce to:

$$V_r = 0$$

$$V_\theta = \Omega r$$

$$V_z = 0$$

and $T = T_o$ (116)

The equations of motion reduce to:

$$\left(\frac{\partial \rho}{\partial z}\right)_{eq} = \rho_{eq} g \approx 0 \tag{117}$$

(The gravitational term may be neglected since it is quite small compared to the centrifugal force.)

$$\left(\frac{\partial p}{\partial r}\right)_{eq} = \rho_{eq} \Omega^2 r = \frac{M}{RT_o} \Omega^2 r p_{eq} \tag{118}$$

Integration of Eq. (118) yields:

$$p_{eq}(r) = p(0) \exp\left[\frac{M\Omega^2}{2RT_o} r^2\right] \tag{119}$$

or

$$\rho_{eq}(r) = \rho(0) \exp\left[\frac{M\Omega^2}{2RT_o} r^2\right] \tag{120}$$

where $p(0)$ and $\rho(0)$ are the pressure and density on the axis, respectively. Equation (120) is identical to Eq. (107).

(3) Linearized Equations of Motion

The quantities in the equations of motion are recast in terms of the perturbations of the equilibrium values due to the internal flow by the transformations:

$$V_r = 0 + u$$
$$V_\theta = \Omega r + v$$
$$V_z = 0 + w \qquad (121)$$

where u, v, and w are the radial, angular, and axial components of the perturbation velocity, and

$$p = p_{eq} + \bar{p}$$
$$\rho = \rho_{eq} + \bar{\rho}$$
$$T = T_o + \bar{T} \qquad (122)$$

where $\bar{p}$, $\bar{\rho}$, and $\bar{T}$ represent the perturbation of the state of the gas due to the internal circulation.

Eqs. (121) and (122) are substituted into the complete equations of motion and any terms which contain the product of two or more perturbation parameters are neglected. This linearization procedure is adequate because the perturbations

due to the internal circulation are small.

The linearized equations of motion are:

overall mass continuity:

$$\frac{1}{r}\frac{\partial}{\partial r}(\rho_{eq} r u) + \frac{\partial}{\partial z}(\rho_{eq} w) = 0 \tag{123}$$

radial momentum:

$$-\bar{\rho} r \Omega^2 - 2\rho_{eq}\Omega v = -\frac{\partial \bar{p}}{\partial r} + \mu\left\{\frac{\partial}{\partial r}\left[\frac{1}{r}\frac{\partial}{\partial r}(ru)\right] + \frac{\partial^2 u}{\partial z^2}\right\} \tag{124}$$

angular momentum:

$$2\rho_{eq}\Omega u = \mu\left\{\frac{\partial}{\partial r}\left[\frac{1}{r}\frac{\partial}{\partial r}(rv)\right] + \frac{\partial^2 v}{\partial z^2}\right\} \tag{125}$$

axial momentum:

$$0 = -\frac{\partial \bar{p}}{\partial z} + \mu\left\{\frac{1}{r}\frac{\partial}{\partial r}\left(r\frac{\partial w}{\partial z}\right) + \frac{\partial^2 w}{\partial z^2}\right\} \tag{126}$$

energy:[7]

$$-\rho_{eq}\Omega^2 r u = \kappa\left[\frac{1}{r}\frac{\partial}{\partial r}\left(r\frac{\partial \bar{T}}{\partial r}\right) + \frac{\partial^2 \bar{T}}{\partial z^2}\right] \tag{127}$$

Equation of State:

$$\bar{\rho} = \left(\frac{M}{RT_o}\right)\bar{p} - \rho_{eq}\left(\frac{\bar{T}}{T_o}\right) \tag{128}$$

Discussion of the boundary conditions on Eqs. (123) - (127) will be postponed until particular solution methods are

described. Some solutions do not consider the presence of the central feed tube while others do. At total reflux, of course, the central feed tube is not essential to the operation of the centrifuge.

In addition to the linearization assumption, another feature which is common to all solutions is the neglect of the gravitational term (i.e., the last term in Eq. (113)). This may at first seem rather odd, since we have referred to the internal circulation induced by unequal plate temperatures as a type of natural convection. In thermal natural convection problems in ordinary flow situations, the acceleration of gravity is a crucial feature of the fluid behavior. In the centrifuge, however, the expansion-compression work term on the left of Eq. (127) replaces the gravitational term as the mechanism by which small temperature inequalities are transformed into fluid motion (see Sec. IIIE.1).

Neglect of the term ρg in the axial equation has an interesting consequence. The system of equations (123) - (127) is invariant to a change in the direction of the z-coordinate. Replacement of z by -z and w by -w does not change the sign of any of the terms in these equations (if a gravitational term were retained in Eq. (126), it would change sign under such a transformation). Thus the system is symmetrical about the midplane at $z=Z/2$, and it should make no difference whether the top plate is heated

and the bottom plate is cooled (as in Fig. 2) or vice versa. This expectation has been confirmed by the experiments of Groth (9).

D. Long Bowl Solutions

If the length of the rotor, Z, is large compared to the radius, the velocity field over a large portion of the centrifuge will be nearly independent of z. Consequently, a class of solutions in which u, v, and w are either functions of radial position only or vary in a simple, prescribed manner with z have been sought. By losing contact with the specific conditions at the end plates of the device, the resulting solutions can only provide a quantity proportional to the axial velocity profile, w(r). Consequently, long bowl solutions provide sufficient information to determine the flow pattern efficiency, E, but not enough to compute m. We first discuss the solution methods employed by various investigators in the long bowl approximation and summarize the results at the end of this section.

(1) Steenbeck (29) and Parker and Mayo (30)

The computational work of Parker and co-workers at the University of Virginia is quite similar in approach to the earlier investigation of Steenbeck (30). Parker's analysis retained terms in the equations of motion which Steenbeck had neglected and introduced the energy equation to properly account for non-isothermality. Solutions obtained by the two studies agree at low peripheral speeds

but differ at high speeds. Only the University of Virginia work will be outlined.

Steenbeck and Parker assume that all of the perturbation quantities in Eqs. (120) and (121) are separable in r and z. If $f_i(r,z)$ denotes any of these parameters, they take:

$$f_i(r,z) = g_i(r)e^{-kz} \tag{129}$$

where $g_i(r)$ is the r-dependent part of the perturbation property, and k is the common eigenvalue (the lowest only), to be determined. After elimination of $\bar{\rho}$ by use of Eq. (128), substitution of Eq. (129) into Eqs. (122) - (127) yields a set of five coupled ordinary differential equations for the radial portions of the perturbation parameters (i.e., the $g_i(r)$ of Eq. (129)), which were solved numerically. The boundary conditions were:

$$\begin{aligned} &\text{at } r=0: && u = \frac{dv}{dr} = \frac{dw}{dr} = \frac{d\bar{T}}{dr} = 0 \\ &\text{at } r=r_2: && u = v = w = 0, \quad \bar{T} = T_o \end{aligned} \tag{130}$$

(the feed tube was assumed absent). The set of differential equations contains the undetermined eigenvalue k, which was also determined in the course of the numerical solution. The perturbation velocity components, u, v, and w, and the fractional departure from isothermality, $\bar{T}/T_o$, were computed

for values of A^2 from 4 to 25. Only relative values of the velocity perturbations could be computed. It was found that the angular and axial perturbation velocity components (v and w) were of the same order of magnitude. Other perturbation quantities (u, $\bar{p}$, and $\bar{T}/T_o$) were several orders of magnitude smaller than v and w. The decay length in the axial direction (i.e., the reciprocal of the first eigenvalue, or k^{-1}) varied from $5000r_2$ to $30r_2$ over the range of A^2 values investigated.

The numerical solution method became increasingly difficult as larger values of A^2 were attempted. Ging (31) has developed an asymptotic solution which avoids this difficulty and agrees well with the numerical solution at $A^2 = 25$.

(2) Soubbaramayer (32)

The first study of Soubbaramayer also ignores the details of the effects at the end plates of the centrifuge and assumes that the velocity perturbations u, v, and w are functions of r only. The pressure perturbation, $\bar{p}$, is eliminated from the linearized equations of motion by taking the partial derivative of Eq. (123) with respect to z and of Eq. (125) with respect to r. The $\partial\bar{\rho}/\partial z$ term appearing in the former as a result of differentiation with respect to z is obtained from Eq. (127). Expressed in terms of the dimensionless radial coordinate $\zeta = r/r_2$, the resulting equation is:

$$2A^2\left[\frac{1}{\zeta}\frac{d}{d\zeta}\left(\zeta\frac{dw}{d\zeta}\right)\right] = Be^{A^2\zeta^2} + \frac{1}{\zeta}\frac{d}{d\zeta}\left[\frac{1}{\zeta}\frac{d}{d\zeta}\left(\zeta\frac{dw}{d\zeta}\right)\right] \qquad (131)$$

where A^2 is given by Eq. (108) and B is a scale factor with units of velocity:

$$B = \frac{r_2^4\Omega^2\rho_{eq}(0)}{\mu T_o}\frac{\partial\bar{T}}{\partial z} \qquad (132)$$

The axial temperature gradient, $\partial\bar{T}/\partial z$, was assumed constant (independent of both r and z) so that the parameter B is also a constant. By dividing Eq. (131) by B, the problem is reduced to a third order ordinary differential equation involving the dimensionless axial velocity

$$W(\zeta) = w(\zeta)/B \qquad (133)$$

Since B is unknown (and cannot be determined at this level of approximation), the solution gives the axial velocity profile to within an undetermined multiplicative factor.

The third order differential equation is supplied with the following boundary conditions

$$W(1) = 0 \qquad \text{(by the no-slip condition)}$$

$$\left(\frac{dW}{d\zeta}\right)_0 = 0 \qquad \text{(by symmetry, since the feed tube was not considered)} \qquad (134)$$

and an integral restriction supplied by the restraint on the flow function expressed by Eq. (99):

$$\int_0^1 e^{A^2\zeta^2} W(\zeta)\zeta d\zeta = 0 \qquad (135)$$

Eq. (131) can be integrated directly (although details of the integration were not given) to yield $W(\zeta)$. The axial velocity profile is parametric in A^2.

(3) Berman (33)

Berman's treatment of centrifuge hydrodynamics is an attempt to obtain the shape of the axial velocity profile without resorting to the extensive numerical computations employed by Parker (30). In keeping with the long bowl model, axial velocity is taken to be a function of radial positions only. The radial and angular components u and v are assumed zero.

In order to sustain an axial velocity profile by Berman's method, a radial temperature gradient is imposed upon the system. The feed tube at $r=r_0$ is taken to be somewhat hotter than the rotor wall at $r=r_2$. Because of this specification, the variation of T with z is neglected. This constitutes a significant departure from Soubbaramayer's approach, in which the axial temperature gradient could not be set equal to zero.

Berman applies these simplifications to the complete set of equations of motion and not to the linearized versions.

The governing equations reduce to:

radial momentum:

$$\frac{\partial p}{\partial r} = \rho r\Omega^2 = \frac{M}{RT}\, pr\Omega^2 \tag{136}$$

axial momentum:

$$\mu\left[\frac{1}{r}\frac{\partial}{\partial r}\left(r\,\frac{\partial w}{\partial r}\right)\right] = \frac{\partial p}{\partial z} + \rho g^* \tag{137}$$

energy:

$$\frac{1}{r}\frac{\partial}{\partial r}\left(r\,\frac{\partial T}{\partial r}\right) = 0 \tag{138}$$

The external force parameter, g* in Eq. (137), does <u>not</u> represent gravity. Rather it is an adjustable driving force for providing the countercurrent flow. In effect, it compensates for the features of the flow lost in the simplification of Eqs. (110) - (114) to the forms shown above.

Since the temperature is assumed to be a function of r only, Eq. (136) shows that:

$$\frac{\partial}{\partial z}\left(\frac{1}{p}\frac{\partial p}{\partial r}\right) = \frac{\partial \ell np}{\partial z \partial r} = \frac{\partial}{\partial r}\left(\frac{\partial \ell np}{\partial z}\right) = 0 \tag{139}$$

or the quantity

$$G = \frac{\partial \ell np}{\partial z} = \frac{1}{p}\frac{\partial p}{\partial z} \tag{140}$$

is a function of z only. Using Eq. (140) and the ideal gas law, Eq. (137) can be written as:

$$\mu\left[\frac{1}{r}\frac{\partial}{\partial r}\left(r\frac{\partial w}{\partial r}\right)\right] = p\left(G + \frac{Mg^*}{RT}\right) \tag{141}$$

where both G and g* are considered as constants.

In order to solve Eq. (141), p is obtained by integration of Eq. (136)

$$p(r) = p(r_0)\exp\left[\frac{M\Omega^2}{R}\int_{r_0}^{r}\frac{r'}{T(r')}\,dr'\right] \tag{142}$$

and T in Eqs. (141) and (142) is determined by direct integration of Eq. (138), which yields:

$$\frac{T(r)}{T_o} = 1 + \left(\frac{T_o - T_2}{T_o}\right)\frac{\ell n(r/r_2)}{\ell n\sigma} \tag{143}$$

where T_o and T_2 are the specified temperatures at the feed tube and the rotor wall, respectively. The ratio r_0/r_2 is denoted by σ. Eq. (141) is thus a second order ordinary differential equation containing two unspecified constants, G and g*. Combining Eqs. (141) and (142) yields:

$$\frac{d}{d\xi}\left[(\xi+\nu)\frac{dw}{d\xi}\right] = B\exp\left\{A^2(1-\sigma^2)\int_0^{\xi}\frac{d\xi'}{[T(\xi')/T_o]}\right\}\left[1 + \frac{\varepsilon}{T(\xi)/T_o}\right] \tag{144}$$

Radial position is expressed by the quantity:

$$\xi = \frac{r^2 - r_0^2}{r_2^2 - r_0^2} \tag{145}$$

B is the velocity scale factor:

$$B = \frac{r_2^2(1-\sigma^2)Gp(0)}{4\mu} \tag{146}$$

and ε is a combination of the constants g* and G:

$$\varepsilon = \frac{M}{RT_o}\frac{g^*}{G} \tag{147}$$

In terms of ξ, the temperature variation with radial position is given by:

$$\frac{T(\xi)}{T_o} = 1 + \left(\frac{T_o - T_2}{T_o}\right)\frac{\ell n(\frac{\xi+\nu}{\nu})}{\ell n\sigma^2} \tag{148}$$

where $\nu = \sigma^2/(1-\sigma^2)$.

Solution of Eq. (144) yields only the dimensionless axial velocity $W(\xi) = w(\xi)/B$, which is analagous to Eq. (133). The boundary conditions reflecting no-slip at the feed tube and rotor wall are:

$$W(0) = W(1) = 0$$

The integral constraint of Eq. (99) is also used. It is:

$$\int_0^1 \exp\left\{A^2(1-\sigma^2)\int_0^{\xi}\frac{d\xi'}{T(\xi')/T_o}\right\} W(\xi)d\xi = 0 \qquad (149)$$

Whereas the Soubbaramayer analysis requires two boundary conditions and the integral constraint because the differential equation is third order, Berman's differential equation is only second order. The integral constraint of Eq. (149) is used to eliminate the undetermined parameter ϵ in Eq. (144).

Berman shows that the solution of Eq. (144) can be reduced to quadrature form; that is, to an equation giving $W(\xi)$ explicitly in terms of integrals over the functions of ξ appearing in Eqs. (144) and (149). These integrals are complex enough to warrant evaluation by computer, for which a program was written (34). Even though numerical computation is still required, the calculations are considerably simpler than the more complete treatment of Parker (30).

Examination of Eqs. (144) and (149) indicates that the solution $W(\xi)$ should depend upon the parameters A^2, $(T_o-T_2)/T_o$, and σ. In fact, however, the profiles are completely insensitive to the last two parameters, provided that they are considerably smaller than unity. This behavior had to occur for a reasonable solution, for the parameter $(T_o-T_2)/T_o$ was imposed upon the problem solely to generate a countercurrent flow. In an actual centrifuge, no attempt is made to regulate feed tube and rotor wall temperatures. In the next section, it will be shown that the artifice of an

imposed radial temperature gradient can be dispensed with, thus permitting a rather simple hand calculation of the velocity profile, the flow function, and the flow pattern efficiency.

(4) Simplified Berman Calculation

The sole reason for specifying a radial temperature gradient in Berman's analysis was to provide a differential equation with enough undetermined parameters to accomodate the two boundary conditions and the integral constraint. If $T(\xi)/T_o$ were set equal to unity in Eq. (144), one of the parameters would be lost (the last bracketed term in Eq. (144) would become $1+\varepsilon$, and the product $B(1+\varepsilon)$ would become the velocity scale factor). Thus, the function of the temperature ratio in the last term on the right in Eq. (144) is simply to provide a radial dependence to this term. The radial variation need not be of the particular form given by $T(\xi)/T_o$ of Eq. (148), but can be chosen in an arbitrary fashion.

Therefore, we begin by: (1) setting the temperature ratio in the exponential term in Eq. (144) equal to unity, (2) assuming $\sigma^2 << 1$, in the same term, and (3) replacing $T_o/T(\xi)$ in the last term on the right by ξ itself (any function of ξ would do; ξ is the simplest). In terms of the dimensionless axial velocity $W=w/B$, Eq. (144) reduces to:

$$\frac{d}{d\xi}\left[(\xi+\nu)\ \frac{dW}{d\xi}\right] = e^{A^2\xi}(1+\varepsilon\xi) \tag{150}$$

subject to the same boundary conditions as in Berman's case. The unknown constant ε is fixed by the restraint:

$$\int_0^1 e^{A^2\xi} W(\xi)\, d\xi = 0 \tag{151}$$

Eq. (150) may be integrated directly to yield:

$$W(\xi) = \frac{Ei[A^2(\xi+\nu)] - Ei(A^2\nu) + \gamma(e^{A^2\xi}-1)}{Ei[A^2(1+\nu)] - Ei(A^2\nu) + \gamma(e^{A^2}-1)} - \frac{\ell n\left(\frac{\xi+\nu}{\nu}\right)}{\ell n\left(\frac{1+\nu}{\nu}\right)} \tag{152}$$

additional ξ-independent factors which appeared in the course of the integrations were incorporated into the velocity scale factor B, which cannot be obtained by this method in any case.

Ei(x) is the exponential integral:

$$Ei(x) = \int_{-\infty}^{x} \frac{e^t}{t}\, dt \tag{153}$$

The exponential integral is tabulated by Jahnke and Ende (35), but convenient asymptotic forms are:

$$Ei(x) = 0.577 + \ln x + \ldots \qquad \text{for small } x \tag{154}$$

and

$$Ei(x) = \frac{e^x}{x-1}\left[1 + \frac{1}{(x-1)^2} + \ldots\right] \text{ for large } x \tag{155}$$

The parameter γ in Eq. (152) is:

$$\gamma = \frac{e^{A^2\nu}}{A^2/\varepsilon - A^2\nu - 1} \tag{156}$$

which is another constant, and shall be determined instead of ε by substitution of Eq. (152) into Eq. (151). For $A^2 > \sim 10$ (which corresponds to a peripheral speed of $\sim$375 m/sec) and $\nu = \sigma^2/(1-\sigma^2)$ between 10^{-4} and 10^{-2} (which corresponds to $0.01 \leq r_o/r_2 \leq 0.1$), the parameter γ is given to a very good approximation by:

$$\gamma = -\frac{2}{2A^2-1} \tag{157}$$

The asymptotic expansion of the exponential integral for large x was used in obtaining Eq. (157).

As it stands, Eq. (152) depends upon A^2 and the geometrical factor ν. Since only the shape of the axial velocity for $\xi > 0.5$ is important in determining the flow function, ν can be eliminated by the following considerations: If $10^{-4} < \nu < 10^{-2}$, then $Ei[A^2(\xi+\nu)] \simeq Ei(A^2\xi)$. If $A^2\xi > \sim 5$, the exponential integral can be approximated by Eq. (155), and $e^{A^2\xi} >> 1$. For the range of ν indicated above, $Ei(A^2\nu)$ may be neglected compared to the other terms in Eq. (152) and the ratio of the logarithms in the right hand term of Eq. (152) may be approximated by unity. Using these approximations, Eq. (152) becomes:

$$W(\xi) = \left(\frac{A^2-1}{A^2\xi-1}\right)[2A^2(1-\xi) + 1]e^{-A^2(1-\xi)} \times$$

$$\left\{\frac{1 + \dfrac{(2A^2-1)}{[2A^2(1-\xi) + 1](A^2\xi-1)^2}}{1 + \dfrac{(2A^2 - 1)}{(A^2-1)^2}}\right\} - 1 \qquad (158)$$

For even larger A^2, the following very simple form results:

$$W(\xi) = \left(\frac{1}{\xi}\right)[2A^2(1-\xi) + 1]e^{-A^2(1-\xi)} - 1 \qquad (159)$$

In terms of the radial variable ξ used in this and in the preceding section, the flow function, to within a constant factor, is:

$$F(\xi) = \int_0^{\xi} e^{A^2\xi'} W(\xi')d\xi' \qquad (160)$$

and the flow pattern efficiency (neglecting σ^2 compared to unity) is:

$$E = \frac{2\left[\int_0^1 F(\xi)d\xi\right]^2}{\int_0^1 [F(\xi)]^2 \frac{d\xi}{\xi}} \qquad (161)$$

The requisite integrations are readily accomplished.

(5) Comparison of the Various Long Bowl Solutions

In this section, we compare the results of the four

long bowl solutions just discussed.

Fig. 12 shows the density-weighted axial velocity profiles for A^2=16 and 25. The ordinate is the integrand of the flow function (see Eq. (160)). The solid circles represent the results of the simplified Berman method, computed from Eq. (159). Agreement between all three solution methods is quite good.

Fig. 13 shows the radial position at which the velocity profiles of Fig. 12 cross zero. All of the simplified models agree well with Parker's results. In general, as the peripheral speed is increased, the zero velocity point approaches the rotor wall, which means that the return upflow is concentrated in a thin layer near the periphery.

Fig. 14 shows a typical flow function for A^2=10 as calculated from Eq. (158) of the simplified Berman model. Note that this curve is quite different from the form $F(\xi)\sim\xi$ required by Eq. (105) for maximum flow pattern efficiency.

The flow pattern efficiencies are plotted on Fig. 15 for the various long bowl models (the two dashed curves result from calculations which will be discussed in the next section). The spot calculations on the simplified long bowl methods agree satisfactorily with the Parker calculation. The latter shows a maximum value of E=0.81 at A^2=5.4.

E. Solutions Which Give Absolute Flow Rates

The solutions discussed in the previous section concentrate on the flow pattern near the midplane of the

centrifuge and disregard the detailed flow effects on the end plates. As a result of this approximation, the shape of the axial flow as a function of radius could be accurately described, but the magnitude of the flow, which depends upon what is happening at the heated and cooled ends, could not be determined.

(1) Martin (36)

The calculations presented by Martin treat the flow field in the neighborhood of the end plates but ignore the presence of the rotor wall. However, because the convective currents are generated at the end plates, knowledge of the hydrodynamics here permits the absolute magnitude of the flow function at all axial positions to be computed.

A sketch of the countercurrent flow in the centrifuge is shown in Fig. 16. The flow near the end plates is primarily radial in direction and is restricted to a thin "boundary layer" on the plates. As the fluid moves in over the top plate, some is turned by 90° and provides the axial flow which was considered in the previous section. A similar phenomenon, but reversed in direction, occurs on the cooled bottom plate.

Martin's analysis starts from the linearized equations of motion. Since the flow is primarily radial in nature, the perturbation components v and w are assumed zero. Since the boundary layer on the plate is assumed to be very

thin, the radial component varies much more rapidly with axial distance z than with r. Thus, Martin assumes that in the equations of motion, only terms which depend upon the variation of u with z are important.

The perturbation quantities of Eq. (122) are restricted as follows:

$$\begin{aligned} \bar{p} &= 0 \\ \bar{\rho} &= \bar{\rho}(z) \\ \bar{T} &= \bar{T}(z) \end{aligned} \tag{162}$$

Applying the simplifications described above to the radial momentum equation, Eq. (124) yields:

$$\mu \frac{d^2u}{dz^2} = -\bar{\rho} r \Omega^2 \tag{163}$$

The angular momentum equation is not considered in Martin's treatment, which immediately introduces an inconsistency. If the angular perturbation velocity component, v, is neglected, Eq. (125) indicates that the term $2\rho_{eq}\Omega u$ (which arises from the Coriolis force) is also negligible, even though this term is of comparable magnitude to the right hand side of Eq. (163).

The energy conservation equation, Eq. (127), becomes:

$$-\rho_{eq} r \Omega^2 u = \kappa \frac{d^2\bar{T}}{dz^2} \tag{164}$$

Eq. (164) shows that the expansion-compression work term (the left hand side) is fundamental to the generation of the flow in the device.

Since $\bar{p}$ has been neglected, the linearized equation of state, Eq. (128), becomes:

$$\bar{T} = -\left(\frac{T_o}{\rho_{eq}}\right)\bar{\rho} \tag{165}$$

These equations are combined to give a single differential equation for the velocity component u as follows: Eq. (163) is differentiated twice with respect to z. The $d^2\bar{\rho}/dz^2$ term which results is proportional to $d^2\bar{T}/dz^2$ by Eq. (165). Finally, $d^2\bar{T}/dz^2$ is eliminated by use of Eq. (164). The resulting fourth order differential equation is:

$$\frac{d^4u}{dz^4} + 4\phi^4 u = 0 \tag{166}$$

where:

$$\phi^4 = \frac{(\frac{1}{2}\rho_{eq} r\Omega^2)^2}{\mu\kappa T_o} \tag{167}$$

The general solution to Eq. (166) is:

$$u = C_1 e^{\phi z}\cos\phi z + C_2 e^{-\phi z}\cos\phi z + C_3 e^{\phi z}\sin\phi z + C_4 e^{-\phi z}\sin\phi z \tag{168}$$

Since we are dealing with a boundary layer type of flow on the end plates, u and all of its derivatives must vanish at large z. Therefore, C_1 and C_3 are zero. At z=0, the no slip condition requires that u(0)=0, so that C_2=0 as well.

The last boundary condition is somewhat less obvious. In the centrifuge, the end plates are held at temperatures which are $2\Delta T$ different from each other (see Fig. 16). The gas far from either end plate is assumed to be at a constant temperature T_o. Therefore, at z=0, $\overline{T}=\Delta T$. Using this condition in Eq. (165) and then in Eq. (163), provides the fourth boundary condition as:

$$\left(\frac{d^2u}{dz^2}\right)_0 = \frac{r\Omega^2\rho_{eq}\Delta T}{\mu T_o} \tag{169}$$

which, when substituted into Eq. (168), permits C_4 to be calculated.

The radial velocity profile in the boundary layer on either end plate is thus given by:

$$u = -\left[\frac{r\Omega^2\rho_{eq}\Delta T}{2\phi^2\mu T_o}\right] e^{-\phi\xi}\sin\phi\xi \tag{170}$$

The profile represented by Eq. (170) is a damped sinusoid, as illustrated in Fig. 17. (The axial distance over which it differs from zero has been greatly expanded for the purpose of illustration.) The "thickness" of the

boundary layer may be taken as the width of the first lobe of the function, which is π/ϕ (the remaining oscillations are rapidly damped out). The maximum radial velocity occurs at $z \sim \pi/4\phi$. Expressing ρ_{eq} as a function of r by Eq. (120) and using the perfect gas law, Eq. (167) may be rearranged to give:

$$\phi^4 = [A^2 \zeta e^{-A^2(1-\zeta^2)}]^2 \frac{p_2^2}{\gamma_2^2 \mu \kappa T_o} \tag{171}$$

where p_2 is the pressure at the periphery, A^2 is given by Eq. (108) and $\zeta = r/r_2$. To avoid condensation of the solid phase of UF_6, p_2 must be less than $\sim$1 atm. Taking p_2=1 atm, r_2=9.3 cm, $\mu = 1.8 \times 10^{-4}$ poise, $\kappa = 1.7 \times 10^{-5}$ cal/cm-sec-°K, T_o=300°K, and A^2=6.5 (corresponding to a peripheral speed of 300 m/sec), ϕ is found to be 20cm^{-1} at a radial position half way between the axis and the periphery. The boundary layer thickness here is thus $\pi/20$=0.16 cm, which is far smaller than any of the other dimensions of the centrifuge. The flow on the end plates is clearly of the boundary layer type.

Eq. (170) and Fig. 17 show that at the heated end plate (ΔT positive), the radial flow is inward and on the cooled end plate (ΔT negative), the flow is outward. The solution obviously begins to break down near the corners of the centrifuge where the end plates join the cylindrical wall of the rotor. Here u begins to change significantly with r and gradients of u with r in the equation of motion

cannot be neglected. The complete neglect of the axial velocity component w also causes difficulties. At radial positions larger than the zero velocity points shown in Figs. 12 and 13, the boundary layer is fed by the upflow portion of the countercurrent. In the core, the boundary layer is depleted of fluid by the downflow in the device. Thus w is not zero in any region of the boundary layer. The Martin solution is also in error because of neglect of the velocity component v, which Parker's analysis (30) showed to be significant.

The flow function $F(\zeta)$, may be computed directly from the radial velocity profile of Eq. (170). Consider a cylindrical surface of radius r attached to the upper (heated) plate. From Fig. 16, it can be seen that all of the inflow across this surface ultimately appears as downflow at axial positions far from the end. The total downflow contained which a radius r is, by the defining equation Eq. (57), equal to the flow function. Thus:

$$F(r) = 2\pi r \rho_{eq}(r) \int_0^\infty u(z)dz \qquad (172)$$

Since the density variation in the axial direction is quite small, $\rho = \rho_{eq} + \bar{\rho}$ has been approximated by ρ_{eq}. Since the integral of $e^{-\phi z}\sin\phi z$ from zero to infinity is $1/2\phi$, insertion of Eq. (170) into Eq. (172) yields:

$$F(\zeta) = K_M \Delta T \sqrt{\zeta}\, e^{\frac{1}{2}A^2\zeta} \tag{173}$$

where:

$$K_M = \left(\frac{2\pi\kappa}{\Omega^2}\right)\left(\frac{p_2^2}{r_2^2 \mu \kappa T_o}\right)^{1/4} (A^2 e^{-A^2})^{1/2} \tag{174}$$

Because the rotor wall does not appear explicitly in Martin's analysis, the flow function of Eq. (173), like the optimum flow function of Eq. (105), does not satisfy the restraint of Eq. (99). However, the flow pattern efficiency may be computed by substituting Eq. (173) into Eq. (63):

$$E = \frac{4\left[\int_0^1 \zeta^{3/2} e^{\frac{1}{2}A^2\zeta^2}\, d\zeta\right]^2}{\int_0^1 e^{A^2\zeta^2}\, d\zeta} \tag{175}$$

which is a function of A^2 only. The pattern efficiencies based upon the Martin profile are plotted in Fig. 15.

The strength of the internal circulation may also be determined from the Martin theory by using Eq. (173) in Eq. (97):

$$m = \frac{K_M \Delta T\left[2\int_0^1 \left[e^{A^2\zeta^2}\, d\zeta\right]^{1/2}\right]}{2\pi\rho D r_2} \tag{176}$$

(2) Soubbaramayer (37)

Soubbaramayer's second approach to the centrifuge problem begins with the linearized equations of motion,

Eqs. (123) - (127), in which the following terms are neglected:

$$\mu \frac{\partial}{\partial r}\left[\frac{1}{r}\frac{\partial}{\partial r}(ru)\right] \qquad \text{in Eq. (124)}$$

$$\mu \frac{\partial}{\partial r}\left[\frac{1}{r}\frac{\partial}{\partial r}(rv)\right] \qquad \text{in Eq. (125)}$$

$$\mu \frac{\partial^2 w}{\partial z^2} \qquad \text{in Eq. (126)}$$

$$\rho_{eq}\Omega^2 ru \text{ and}$$

$$\kappa\left[\frac{1}{r}\frac{\partial}{\partial r} r \frac{\partial \bar{T}}{\partial r}\right] \qquad \text{in Eq. (127)}$$

In terms of the radial variable $\zeta = r/r_2$ and the dimensionless axial variable

$$s = z/r_2 \tag{177}$$

the equations of motion become:

overall continuity (after using Eq. (120):

$$\frac{\partial u}{\partial \zeta} + (\frac{1}{\zeta} + 2A^2\zeta)u + \frac{\partial w}{\partial s} = 0 \tag{178}$$

radial and axial momentum (after eliminating $\bar{p}$):

$$\frac{\Omega r_2}{2T_o}\frac{\partial \bar{T}}{\partial s} = \frac{e^{A^2(1-\zeta^2)}}{Re}\left\{2A^2\frac{1}{\zeta}\frac{\partial}{\partial \zeta}\left(\zeta\frac{\partial}{\partial \zeta}\right) - \frac{1}{\zeta}\frac{\partial}{\partial \zeta}\left[\frac{1}{\zeta}\frac{\partial}{\partial \zeta}\left(\zeta\frac{\partial}{\partial \zeta}\right)\right] + \frac{1}{\zeta}\frac{\partial^3 u}{\partial s^3}\right\} + \frac{1}{\zeta}\frac{\partial v}{\partial s} \tag{179}$$

where Re is a type of Reynolds number:

$$Re = \frac{2\rho_{eq}(r_2)\Omega r_2^2}{\mu} \tag{180}$$

(note that Eq. (179) reduces to Eq. (131) if u and v are assumed independent of s, as in Soubbaramayer's long bowl analysis.)

angular momentum:

$$e^{-A^2(1-\zeta^2)}u = \frac{1}{Re}\frac{\partial^2 v}{\partial s^2} \tag{181}$$

energy:

$$\frac{\partial^2 \bar{T}}{\partial s^2} = 0 \tag{182}$$

The boundary conditions are (by symmetry, only the top half of the centrifuge is considered):

at $z=0$: $u=v=w=0$, $\bar{T}=\Delta T(\zeta)$ (183a)

$\Delta T(\zeta)$ is a specified temperature profile along the end plate.

at $z=Z/2$: $u=v=\partial w/\partial z=\bar{T}=0$ (183b)

at $r=0$: $u=v=\partial w/\partial r=0$ (184a)

at $r=r_2$: $u=v=w=0$ (184b)

Note that the v boundary condition at r=0 is not the same as Parker's (Eq. (130)).

A trial function of the following form is selected:

$$u = (\Omega r_2) g(\zeta) e^{-\psi s} \sin\psi s \tag{185}$$

where ψ is a function of ζ only and is given by:

$$\psi = \left\{ \frac{1}{2} \text{ Re } e^{-A^2(1-\zeta^2)} \right\}^{1/2} \tag{186}$$

The profile of Eq. (185) is of the same damped sinusoidal form as was obtained by Martin, Although the coefficient ψ is not equivalent to Martin's ϕ (Eq. (171)).

The trial function given by Eq. (185) is substituted for u in Eqs. (178) and (181). Since ψ is very large (because Re is large), terms containing $e^{-\psi s}$ are neglected and one obtains:

$$v = -(\Omega r_2) g(\zeta) \left[1 - \frac{s}{(Z/2r_2)} \right] \tag{187}$$

$$w = -\frac{(\Omega r_2)}{2\psi} \left[\frac{dg}{d\zeta} + g\left(\frac{1}{\zeta} + 2A^2\zeta - \frac{1}{\psi} \frac{d\psi}{d\zeta} \right) \right] \tag{188}$$

The temperature perturbation is obtained by direct integration of Eq. (182):

$$\overline{T} = \Delta T(\zeta) \left[1 - \frac{s}{(Z/2r_2)} \right] \tag{189}$$

In their full form (i.e., $e^{-\psi s}$ terms included), Eqs. (187) and (188) satisfy the z=0 Boundary conditions of Eq. (183a). Ignoring terms containing $e^{-\psi s}$ restricts the solution to regions far from the ends. In particular, the axial velocity of Eq. (188) is independent of s (or z), and hence w is a long bowl type of solution. However, Soubbaramayer claims that by keeping the solution general enough to satisfy the z boundary condition up to this point, the end effects are not neglected as in the true long bowl methods. Indeed, the solution presented by Soubbaramayer does permit absolute magnitudes of the axial velocity to be computed.

The function $g(\zeta)$ is obtained as the solution to the differential equation which results from substituting Eqs. (187)-(189) into Eq. (179) (the s-dependence in the last two terms of Eq. (179) cancel provided that the form of Eq. (187) which includes $e^{-\psi s}$ is utilized). Only the highest order derivative with respect to ζ is retained in the first and second terms on the right of Eq. (179). The resulting fourth order differential equation for $g(\zeta)$ is:

$$\zeta \frac{\Delta T(\zeta)}{T_o} + 2g(\zeta) + \frac{1}{4} \frac{(Z/r_2)}{\psi^3} \frac{d^4 g}{d\zeta^4} = 0 \qquad (190)$$

subject to the boundary conditions:

$$g(0) = \left(\frac{d^2 g}{d\zeta^2}\right)_0 = 0$$
$$g(1) = \left(\frac{dg}{d\zeta}\right)_1 = 0 \qquad (191)$$

Eq. (190) was solved numerically for the set of conditions:

p_2 = 30 cm Hg

ΔT = 10°C (constant with radius)

Ωr_2 = 300 m/sec

r_2 = 11.5 cm

Z = 140 cm

T_o = 340°K

(these conditions correspond to A^2=5.6).

The axial velocity profile is shown in Fig. 18. Two aspects of this curve are significant. First, the zero velocity point occurs at $\zeta \simeq 0.97$, which falls far from the curve of Fig. 13 representing the true long bowl solutions. Second, the maximum axial velocity is $\sim$10 cm/sec, which is indeed small compared to the peripheral speed of 30,000 cm/sec.

The flow function corresponding to the velocity profile of Fig. 18 is depicted in Fig. 19 along with the Martin flow function (Eq. (173)) for the same conditions (i.e., K_M = 2150 kg/hr). The two flow functions disagree by nearly two orders of magnitude. However, the Soubbaramayer flow function is zero at the periphery, as required by the restraint of Eq. (99).

Because the coefficient of the fourth order derivative in Eq. (190) is very small, the last term in Eq. (190)

is negligible except for regions very near to the wall. Therefore, integrals of the flow function required for the pattern efficiency E and the internal flow magnitude parameter m can be accurately computed using the approximation:

$$g(\zeta) \simeq -\frac{1}{2}\frac{\Delta T(\zeta)}{T_o}\zeta \tag{192}$$

from which the axial velocity may be obtained with the aid of Eq. (188).

To this approximation, the flow pattern efficiency for ΔT=constant is given by:

$$E = \frac{32}{A^4}\frac{\left[(\frac{1}{2}A^2-1)e^{\frac{1}{2}A^2}+1\right]^2}{(A^2-1)e^{A^2}+1} \tag{193}$$

which, in common with the long bowl solutions discussed in Sec. IIID, depends only upon A^2. Eq. (193) is graphed on Fig. 15. It does not agree with either the Martin or the true long bowl results.

The internal circulation parameter of Eq. (97) can also be determined from the results. For ΔT=constant, it is:

$$m = \frac{(A^2-1)^{1/2}}{2^{3/2}A}\left(\frac{\mu}{\rho D}\right)\frac{\Delta T}{T_o}\left(\frac{p_2}{\Omega\mu}\right)^{1/2} \tag{194}$$

(the group $\mu/\rho D$ is the Schmidt number, which is approximately 0.75 for UF_6). Eq. (194) and the Martin result, Eq. (176), are in significant disagreement, both in form and in magnitude.

IV. CONCLUSION

The separative analysis of the thermally driven counter-current gas centrifuge is well understood. The physical properties of the uranium hexafloride process gas are reasonably well known. Simple analytic forms formulae for the optimum separative power, separation factor and throughput are available. These results are valid up to peripheral speeds of ∿300 m/sec, where the close separation approximations to the separation factor (Sec. II-I) and the separative power (Eq. (11)) begin to fail. At high peripheral speeds, the separation factor becomes significantly larger than unity. In this case, the analysis becomes more complicated but in principal poses no difficulties. The separative power at large α has been discussed by Cohen (18), Ouwerkerk and Los (24), and Bulang et al (25).

The simple analysis assumes that the throughput is small compared to the internal circulation, but this restriction may also be relaxed (24,23).

The separative properties of the centrifuge depend upon two fluid mechanical characteristics of the device, the flow pattern efficiency E and the internal circulation parameter m. Both of these parameters depend upon double integrals of the axial velocity profile. The efficiency E requires knowledge of the shape of the velocity profile. In addition, calculation of m is possible only if the magnitude and shape of the axial velocity profile are known.

The long bowl analyses (Sec. IIID) provide a satisfactory (although not yet experimentally verified) prediction of E, which depends only upon the parameter A^2. Parker's analysis (30) appears to be the soundest. The two known attempts to obtain complete velocity profiles are in substantial disagreement, and this problem needs further study. Experimental investigation of the flow inside a centrifuge is essentially impossible, because of the extreme difficulty of installing and extracting information from measuring devices inside the spinning rotor. Hydrodynamic studies will undoubtedly continue to be theoretical. A major theoretical obstacle is encountered in the hydrodynamic analysis of centrifuges operating at high peripheral speeds. Because UF_6 remains gaseous only at pressures less than one atm at room temperature, high speeds will result in very low pressures on the axis. The axial pressure may be so low that the gas here is in the free molecule flow regime. If so, the hydrodynamic analysis must treat an extraordinarily difficult problem involving rarefied gas dynamics in the core coupled to continuum fluid mechanics near the periphery.

Acknowledgment

The author would like to thank the Commissariat à l'Energie Atomique for providing information on recent French centrifuge work.

Part of this study was conducted under the auspices of the U.S. Atomic Energy Commission.

APPENDIX

HYDRODYNAMIC DERIVATION OF THE MAXIMUM SEPARATIVE POWER OF A CENTRIFUGE

The maximum possible separative power of any centrifuge has been presented by Cohen (ref. 18, pp. 20-21, 109-110). Here we derive the same quantity by a somewhat different method, but one which is more in keeping with the hydrodynamic spirit in which the other processes occuring in the centrifuge are treated.

The "value" may be regarded as a local property of the fluid, in the same sense as thermodynamic variables such as entropy or internal energy. The value of the fluid at a particular point, however, is dependent only upon isotopic composition by Eq. (10). As for local thermodymamic properties, it is possible to write a conservation statement for the value in the moving fluid. The "value transport equation" so obtained is very similar to the entropy transport equation which plays a fundamental role in nonequilibrium thermodynamics.

A general conservation equation can be derived for any intensive property of a moving fluid (ref.38, p. 9). When applied to the property we have called the value, it takes the form:

$$\frac{\partial(CV)}{\partial t} + \nabla\cdot\underline{N}_v = R_v \qquad \text{(A-1)}$$

In Eq. (A-1), C is the total concentration of the fluid, V is the value of a unit amount of fluid and $\underline{N}_V$ is the vector flux of value. The rate of production of value per unit volume of fluid is denoted by R_V. This quantity is related to the separative power of the unit by:

$$\delta U = \int_0^{r_2} 2\pi r dr \int_0^{Z} dz R_V \qquad \text{(A-2)}$$

Eq. (A-1) is entirely analogous to the common species conservation relation, Eq. (16), except that there is no production term in the latter (at least not in the case of the centrifuge).

Just as in the transport of matter, the transport of value can be broken up into a diffusive term $\underline{J}_V$ and a convective term:

$$\underline{N}_V = \underline{J}_V + C\underline{v}V \qquad \text{(A-3)}$$

which is the value analog of Eq. (17).

Inserting Eq. (A-3) into Eq. (A-1) yields:

$$C \frac{\partial V}{\partial t} + C\underline{v}\cdot\nabla V + \nabla\cdot\underline{J}_V = R_V \qquad \text{(A-4)}$$

where the overall mass continuity equation:

$$\frac{\partial C}{\partial t} + \nabla\cdot(C\underline{v}) = 0 \qquad \text{(A-5)}$$

has been used (we have assumed that the average molecular weight of the fluid is everywhere uniform, so that total mass density ρ and total molar density C are related by the constant average molecular weight). Eq. (A-4) is the value analog of Eq. (18).

We now need to develop an expression for the diffusive component of the value flux, $\underline{J}_V$. The property called value does not "diffuse" in the same sense that molecules diffuse (according to Fick's law) or heat diffuses (according to Fourier's law). Rather, value is transported due to the interdiffusion of the two isotopic species in the gas, which are denoted by A and B. The value flux due to molecular transport by diffusion may be expressed by:

$$\underline{J}_V = \underline{J}_A \overline{V}_A + \underline{J}_B \overline{V}_B \qquad \text{(A-5)}$$

where $\underline{J}_A$ and $\underline{J}_B$ are the diffusive components of the matter fluxes as employed in Sec. IIA. By analogy to energy transport by interdiffusion in multicomponent systems (ref. 19, p. 566) and entropy transport in a moving fluid (ref. 38, Eq. (3-32)), the quantities $\overline{V}_A$ and $\overline{V}_B$ are identified with <u>partial molal values</u> (in the transport of energy, $\overline{V}_A$ and $\overline{V}_B$ are replaced in Eq. (A-5) by the partial molal enthalpies of A and B; in the transport of entropy, $\overline{V}_A$ and $\overline{V}_B$ become partial molal entropies). The partial molal value is defined as follows: Consider a volume of fluid containing n_A moles of A and n_B moles of B. The total value of this region of fluid is:

$$V_{tot} = (n_A+n_B)V(x_A) \tag{A-6}$$

where V is the value function of Eq. (10) and x_A is the mole fraction of component A:

$$x_A = \frac{n_A}{n_A+n_B} \tag{A-7}$$

Like any other partial molal quantity, the partial molal value of components A and B are given by:

$$\bar{V}_A = \left(\frac{\partial V_{tot}}{\partial n_A} \right)_{n_B} \tag{A-8}$$

and

$$\bar{V}_B = \left(\frac{\partial V_{tot}}{\partial n_B} \right)_{n_A} \tag{A-9}$$

Inserting Eqs. (A-6) and (A-7) into Eqs. (A-8) and (A-9) yields:

$$\bar{V}_A = V(x_A) + (1-x_A)(dV/dx_A) \tag{A-10}$$

$$\bar{V}_B = V(x_A) - x_A(dV/dx_A) \tag{A-11}$$

Substituting Eqs. (A-10) and (A-11) into Eq. (A-5) results in:

$$\underline{J}_V = \underline{J}_A \left(\frac{dV}{dx_A} \right) \tag{A-12}$$

where we have used the fact that $\underline{J}_A+\underline{J}_B = 0$ (ref. 19, p. 501; ref. 38, Eq. (1-11)). The divergence of $\underline{J}_V$ is:

$$\nabla\cdot\underline{J}_V = \nabla\cdot\left[\underline{J}_A\left(\frac{dV}{dx_A}\right)\right] = \left(\frac{dV}{dx_A}\right)\nabla\cdot\underline{J}_A + \underline{J}_A\cdot\nabla\left(\frac{dV}{dx_A}\right) \qquad \text{(A-13)}$$

Since the value function depends only upon composition x_A, the gradient of V or its derivative may be expressed by:

$$\nabla V = \left(\frac{dV}{dx_A}\right)\nabla x_A \qquad \text{(A-14)}$$

$$\nabla\left(\frac{dV}{dx_A}\right) = \left(\frac{d^2V}{dx_A^2}\right)\nabla x_A \qquad \text{(A-15)}$$

Substituting Eqs. (A-12) - (A-14) into Eq. (A-4) yields:

$$R_V = \underline{J}_A\cdot\nabla x_A\left(\frac{d^2V}{dx_A^2}\right) + \left[C\frac{\partial x_A}{\partial t} + C\underline{v}\cdot\nabla x_A + \nabla\cdot\underline{J}_A\right]\left(\frac{dV}{dx_A}\right) \qquad \text{(A-16)}$$

If Eq. (18) is expanded and use made of the overall continuity equation, Eq. (A-5), the bracketed coefficient of dV/dx_A in Eq. (A-16) is seen to be identically zero. Computing the second derivative of the value function from Eq. (10) and omitting the subscript A on the mole fraction symbol, Eq. (A-16) reduces to:

$$R_V = \frac{\underline{J}_A\cdot\nabla x}{[x(1-x)]^2} \qquad \text{(A-17)}$$

which is the desired form of the value transport equation

in a moving fluid. Eq. (A-17) is equivalent to the formula given by Cohen (Eq. 6.21 of ref. 18) and is identical to the formula used by Bock (28).

The value transport equation can be specialized for the centrifuge (any centrifuge, not just the counter current type) by inserting the appropriate expression for $\underline{J}_A$. Using Eqs. (38) and (39) for the radial and axial components of $\underline{J}_A$ in Eq. (A-16) and rearranging yields:

$$-\frac{R_V[x(1-x)]^2}{CD} = \left\{[2a^2x(1-x)r] + \frac{\partial x}{\partial r}\right\}\left(\frac{\partial x}{\partial r}\right) + \left(\frac{\partial x}{\partial z}\right)^2 \quad \text{(A-18)}$$

We now regard the gradients $\partial x/\partial r$ and $\partial x/\partial z$ as variables and the term $2a^2x(1-x)r$ as a constant. The left hand side of Eq. (A-18) is maximized with respect to both $\partial x/\partial r$ and $\partial x/\partial z$. The maximum occurs at:

$$(\partial x/\partial z)_{\max R_V} = 0 \quad \text{(A-19)}$$

$$(\partial x/\partial r)_{\max R_V} = -a^2x(1-x)r \quad \text{(A-20)}$$

The radial concentration gradient which maximizes the separative power per unit volume (Eq. (A-20) is thus one half of the equilibrium gradient (Eq. (46)).

Inserting Eqs. (A-19) and (A-20) into Eq. (A-17) yields:

$$(R_V)_{\max} = CDa^4r^2 \quad \text{(A-21)}$$

If this value production rate is sustained at all points in the centrifuge, Eq. (A-20) may be used in Eq. (A-2) and the latter integrated over the entire centrifuge, which yields:

$$\delta U_{max} = \frac{1}{4}(2\pi CDr_2)\left[a^2 r_2^2\right]^2\left(\frac{Z}{r_2}\right) \qquad \text{(A-22)}$$

FOOTNOTES

[1]The stages must be interconnected to avoid mixing of streams of different compositions. For example, for $\theta=1/3$, the heads streams must be brought forward two stages instead of to the next stage as in a cut -1/2 cascade.

[2]A species conservation equation may be written for both components of a binary mixture. However, the sum of the two species conservation equations is equal to the overall continuity equation. Thus, only one of the two species continuity equations in a binary mixture is independent.

[3]Because of the proximity of the molecular weights of the species $U^{235}F_6$ and $U^{238}F_6$, we need not worry about the distinction between the "mass average" and "mole average" velocities (19). The momentum equations, being statements of Newton's second law, provide the mass average velocity of the fluid. Use of molar units in Eq. (17) implies that $\underline{v}$ in this equation is the mole average velocity. We do not correct for this minor effect.

[4]Another common example of the distribution of molecular species in a force field is the variation of density of air with altitude above the earth. In this case, the force is -mg and the potential energy is mgz, where z is the height above ground. Since the Boltzmann factor is proportional to the density, $\rho(z) = \rho(0)\exp(-Mgz/RT)$, which is the "law of atmospheres".

[5]This is analagous to the situation concerning the fundamental thermodynamic formula $dU = TdS + pdV$, which, although derived by considering a reversible process, is valid for irreversible processes as well.

[6]Throughout this section, the total concentration C will be replaced by the total mass density $\rho(\rho=MC)$. The flow function of Eq. (57) and the diffusion factor in the denominator of Eq. (97) have units of mass per unit time.

[7]In simplifying the expansion-compression work term in Eq. (114), use has been made of overall continuity and the fact that for an ideal gas, $(\partial p/\partial T)_\rho = p/T$.

REFERENCES

1. Nuclear News, 12, 9 (Jan. 1969).

2. The Wall Street Journal, Wed., June 3 (1970).

3. C.F. Barnaby, Science Journal, 5A, 54 (1969).

4. FORATOM study A European Enrichment Plant, Nucl. Eng. Int'l, 14, 343 (1969).

5. M. Bogaardt and F.H. Theyse, in the Symposium on the Problems in the Separation of Uranium Isotopes, Turin, Italy, Oct. 1-2 (1968).

6. J. Kistemaker, J. Los and E.J.J. Veldhuyzen, U.N. Conf. on the Peaceful Uses of At. En., 4, 435 (1958).

7. E.W. Becker, Nuclear News, 12, 46 (July 1969).

9. Bourgain, LeManach, and Berthoumieux, Symposium on the Problems in the Separation of Uranium Isotopes, Turin Italy, Oct. 1-2 (1968).

9. W. Groth in Separation of Isotopes, H. London, Ed., Chap. 6, George Newnes, Ltd., London (1961).

Sep'n, Amsterdam, p. 667, North Holland Publishing Co. (1958).

11. W.E. Groth, K. Beyerle, E. Nann, and K.H. Welge, U.N. Conf. on the Peaceful Uses of At. En., 4, 439 (1958).

12. W. Groth and K.H. Welge, Z. fur Phys. Chem., 19, 1 (1959) (AEC-tr-4264).

13. J.J. Barker, U.S. AEC Report NYO-7348 (1956).

14. H. Martin, Chem. Ingr. Tech., 31, 73 (1959) (NP-tr-493).

15. G. Zippe, U.S. AEC Report ORO-315 (1960).

16. J. Shacter, E. von Halle, and R.L. Hoglund, Kirk-Othmer Encl. of Chem. Tech., 2nd Ed., 7, 148 (1965).

17. J.W. Beams, L.B. Snoddy, and A.R. Kuhlthau, U.N. Conf. on the Peaceful Uses of At. En., 4, 428 (1958).

18. K.P. Cohen, The Theory of Isotope Separation as Applied to the Large Scale Production of U-235, McGraw-Hill, New York (1951).

19. R.B. Bird, W.E. Stewart, and E.N. Lightfoot, Transport Phenomena, Wiley, New York (1960).

20. F. Reif, Fundamentals of Statistical and Thermal Physics, pp. 210-211, McGraw-Hill, New York (1965).

21. J. Los, Z. Naturf, 19A, 106 (1964).

22. A. Kanagawa and Y. Oyama, J. At. Energy Soc. Japan, 3, 868 (1961) (AEC-tr-5135) and Nippon Genshiryoku Gakkaishi 3, 918 (1961) (AEC-tr-5136).

23. A.S. Berman, U.S. AEC Report K-1536 (1962).

24. C. Ouwerkerk and J. Los, UN Conf. on the Peaceful Uses of At. En., 12, 367 (1964).

25. W. Bulang, W. Groth, I. Jordan, W. Kolbe, E. Nann, and K.H. Welge, Z. fur Phys. Chem. 24, 249 (1960) (AEC-tr-4349).

26. R. Courant and D. Hilbert, Methods of Mathematical Physics, Vol. I, p. 49, Interscience, New York (1953).

27. J. Los and J. Kistemaker, Proc. of the Symposium on Isotope Separation, Amsterdam, p. 695, North Holland Publishing Co. (1958).

28. I.E. Bock, Z. Naturf., 18a, 465 (1963).

29. M. Steenbeck, Kernenergie 1, 921 (1958).

30. H.M. Parker and T.T. Mayo, U.S. AEC Report UVA-279-63U (1963).

31. J. Ging, U.S. AEC Report UVA-198-62S (1962).

32. M. Soubbaramayer, CEA Internal Report GC - 588 (1961).

33. A.S. Berman, U.S. AEC Report K-1535 (1963).

34. A.A. Brooks, U.S. AEC Report K-1537 (1962).

35. E. Jahnke and F. Emde, Tables of Functions, p. 1-9, 4th Ed., Dover, New York (1945).

36. H. Martin, Z. fur Elektrochemie 54, 120 (1950) (AEC-tr-3170).

37. M. Soubbaramayer, CEA Internal Report GC-601 (1961) (the results of this work are summarized in ref. 8).

38. D.D. Fitts, Nonequilibrium Thermodynamics, McGraw-Hill, New York (1962).

FIGURE CAPTIONS

1. Gas centrifuge with externally maintained countercurrent. Beams (17), modified for enricher operation.
2. Thermally driven countercurrent centrifuge. Groth (9)
3. A single separating unit
4. An ideal cascade
5. Simplified picture of molecular transport in a gas
6. Particle in a spinning fluid
7. Schematic of a thermally driven gas centrifuge
8. Perturbation of the axial velocity profile set up by natural convection due to introduction of feed and withdrawal of product and waste
9. Variation of the separation factor at total reflux with the strength of internal circulation
10. Effect of internal circulation on the separation factor for different feed flow rates. (θ fixed)
11. Effect of throughput on the separation factor at the optimum internal circulation rate. (θ fixed)
12. Density-weighted axial velocity profiles
13. Dimensionless radial position at which W=0
14. The flow function for $A^2=10$
15. Dependence of the flow pattern efficiency on the parameter A^2 for various solution methods
16. Schematic of streamlines in a thermally driven gas centrifuge, showing regions where the long bowl and the Martin solutions apply

17. Radial velocity component according to the Martin analysis.
18. Axial velocity profile away from the end plates as calculated by Soubbaramayer.
19. Flow functions according to Martin and Soubbaramayer.

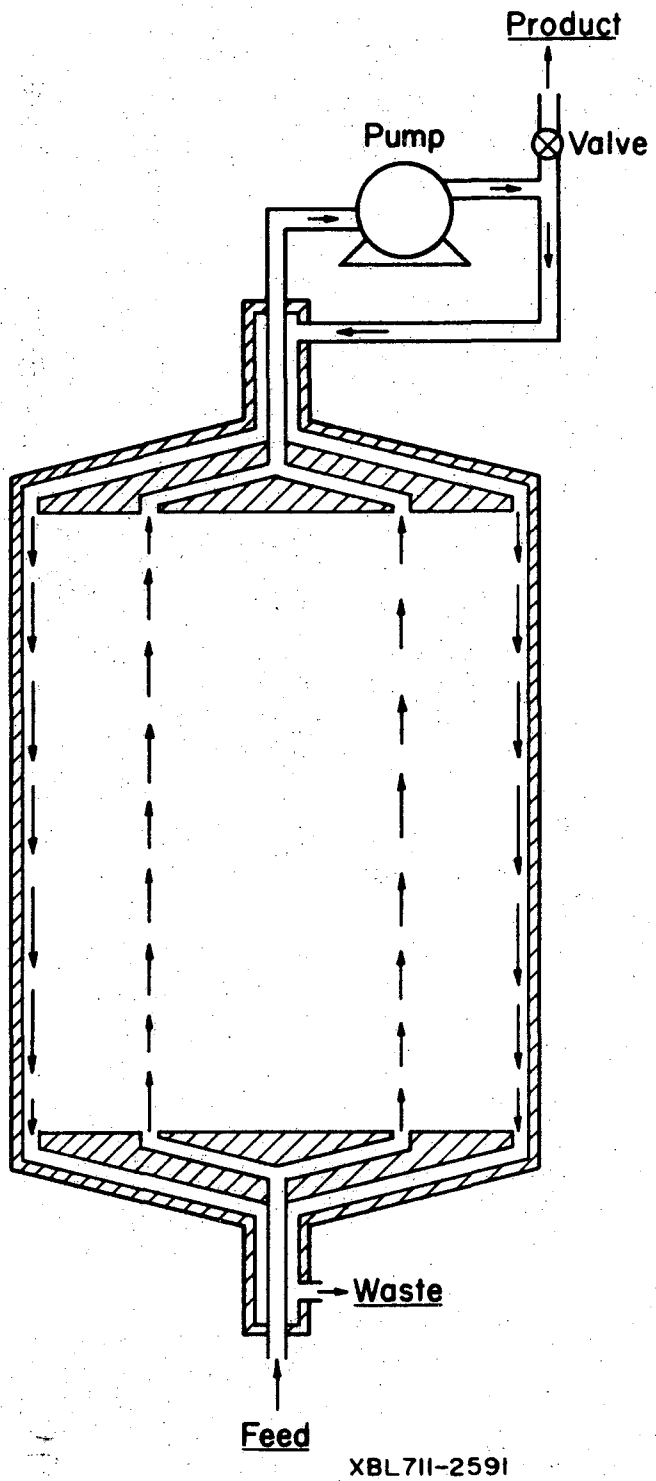

Fig. 1

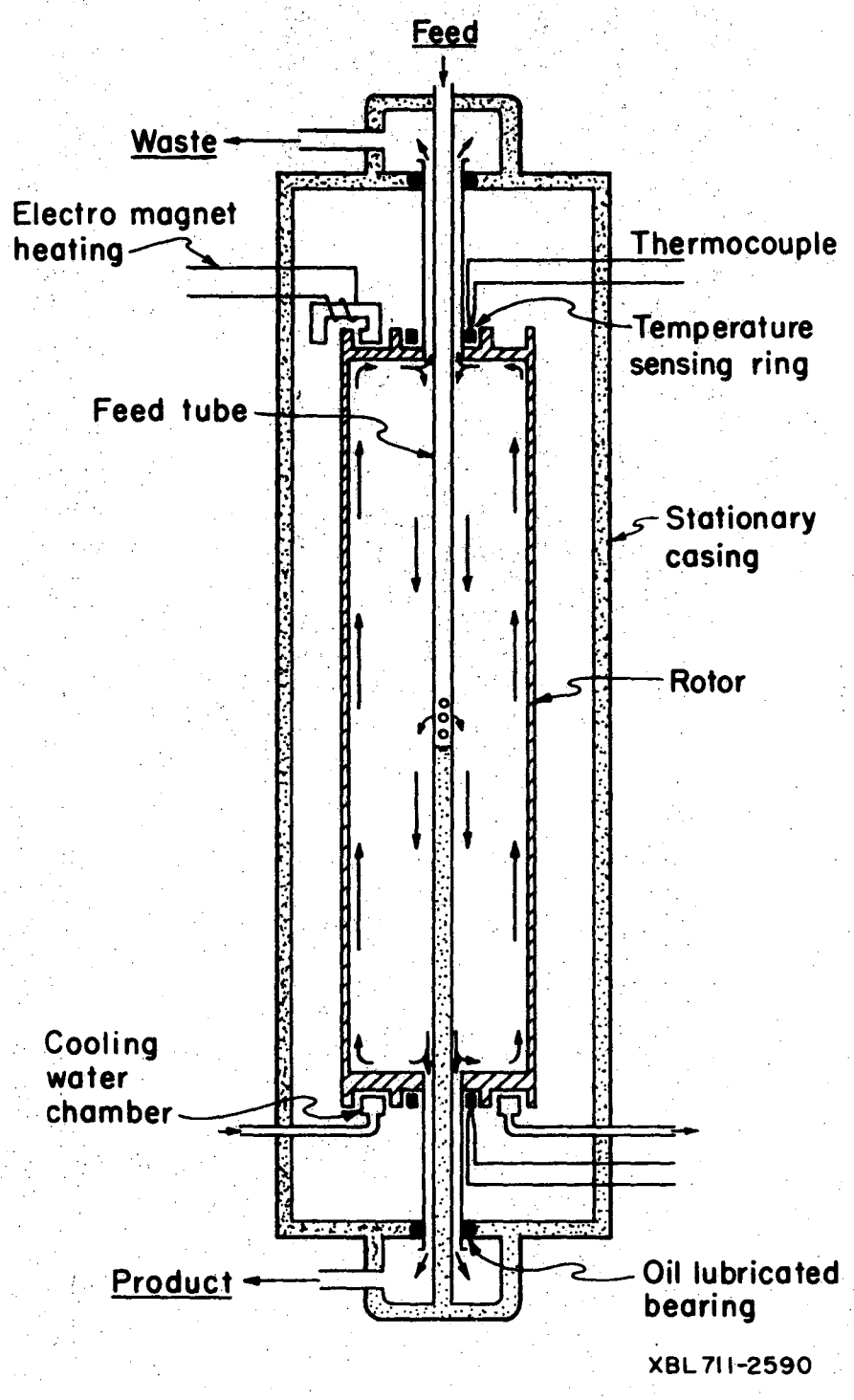
Feed
Waste
Electro magnet heating
Thermocouple
Temperature sensing ring
Feed tube
Stationary casing
Rotor
Cooling water chamber
Product
Oil lubricated bearing
XBL 711-2590

Fig. 2

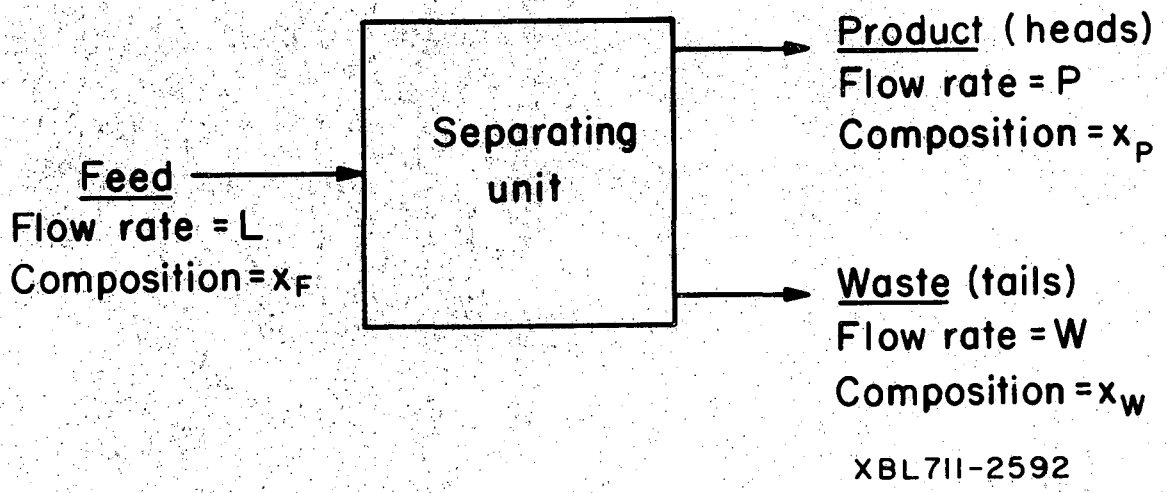
Feed
Flow rate = L
Composition = x_F
Separating unit
Product (heads)
Flow rate = P
Composition = x_P
Waste (tails)
Flow rate = W
Composition = x_W
XBL711-2592

Fig. 3

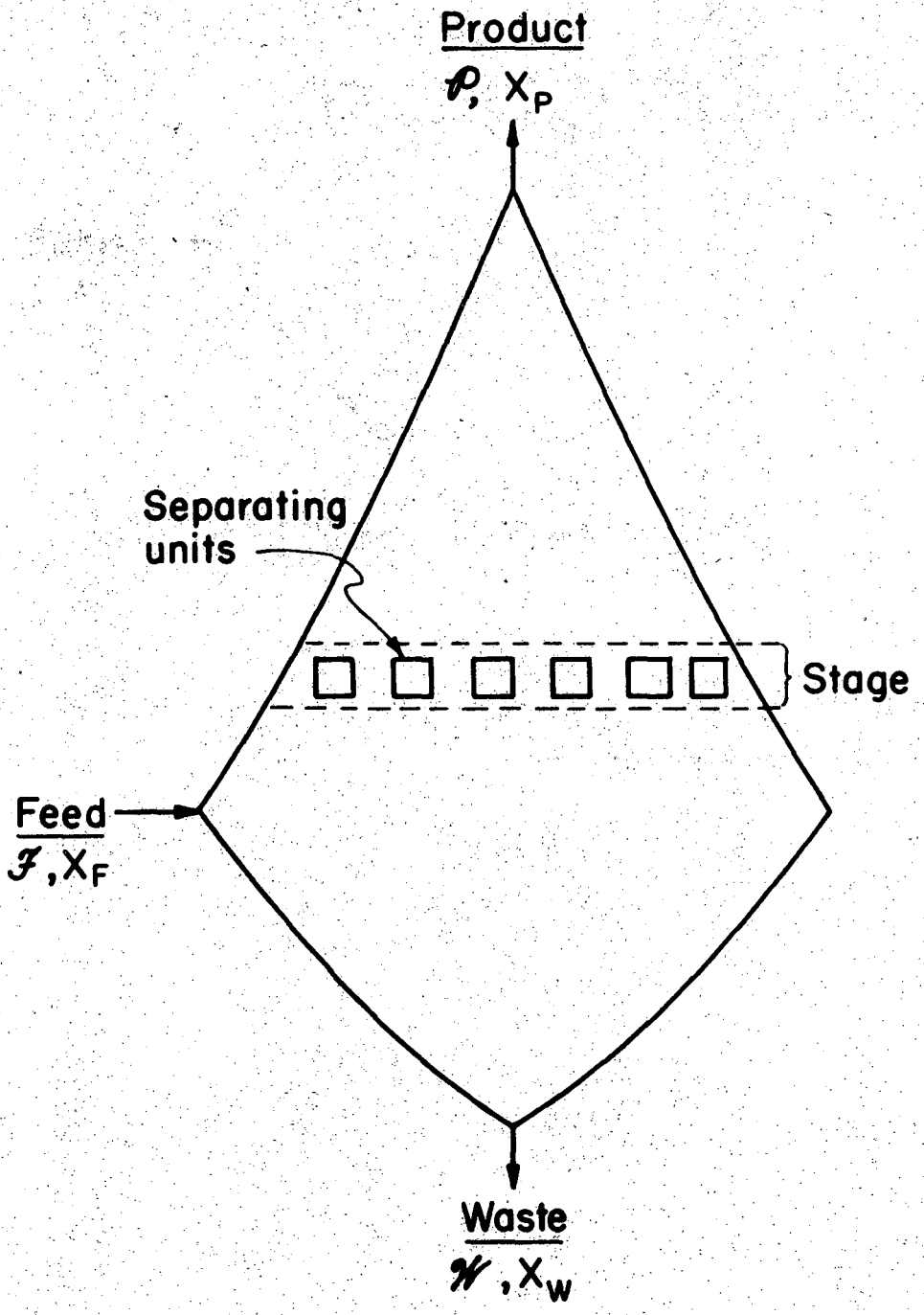
Product
$\mathcal{P}$, X_P
Separating units
Stage
Feed
$\mathcal{F}$, X_F
Waste
$\mathcal{W}$, X_W
XBL711-2593

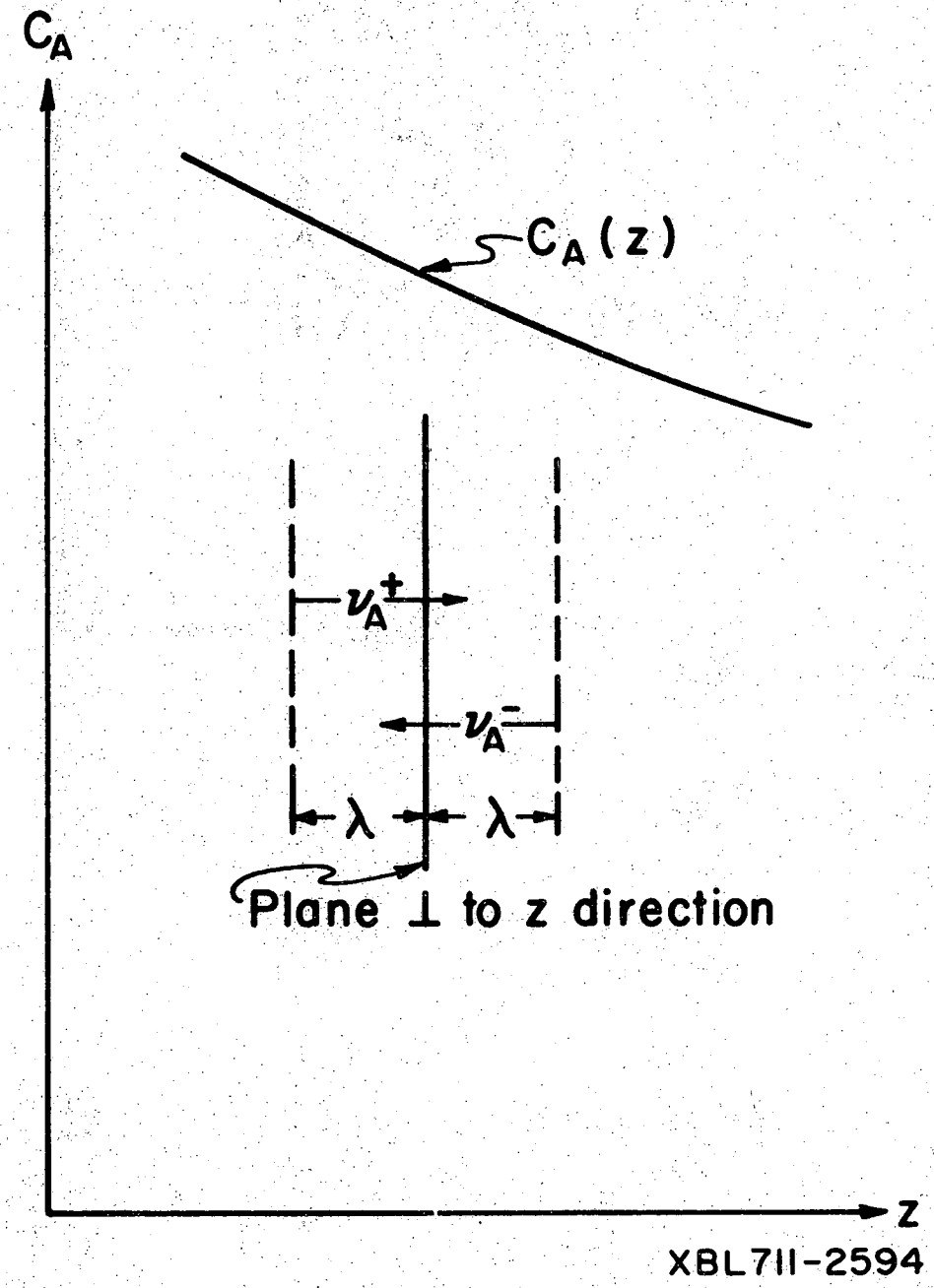
C_A
$C_A(z)$
ν_A^+
ν_A^-
λ
λ
Plane ⊥ to z direction
z
XBL711-2594

Fig. 5

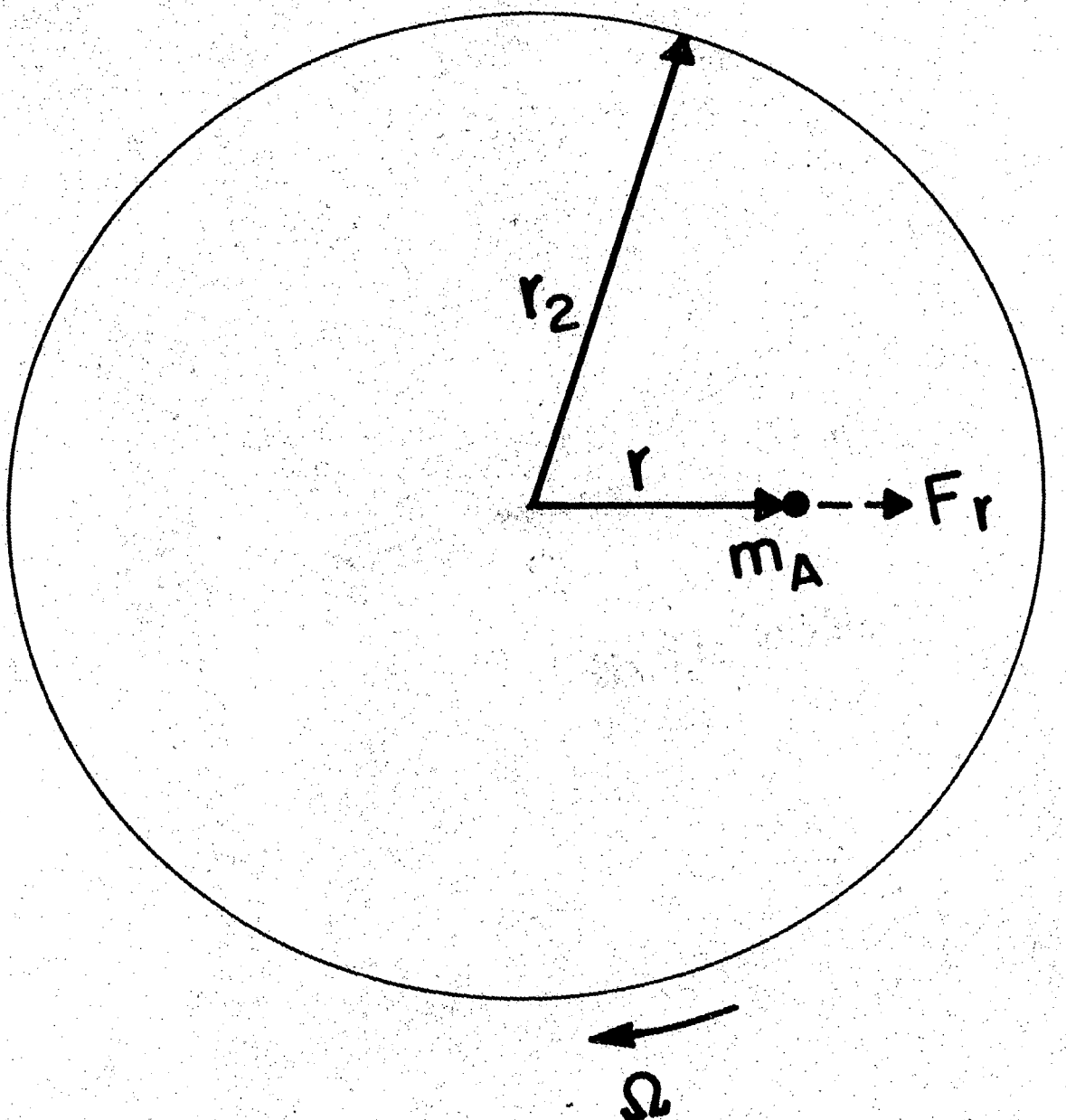

Fig.

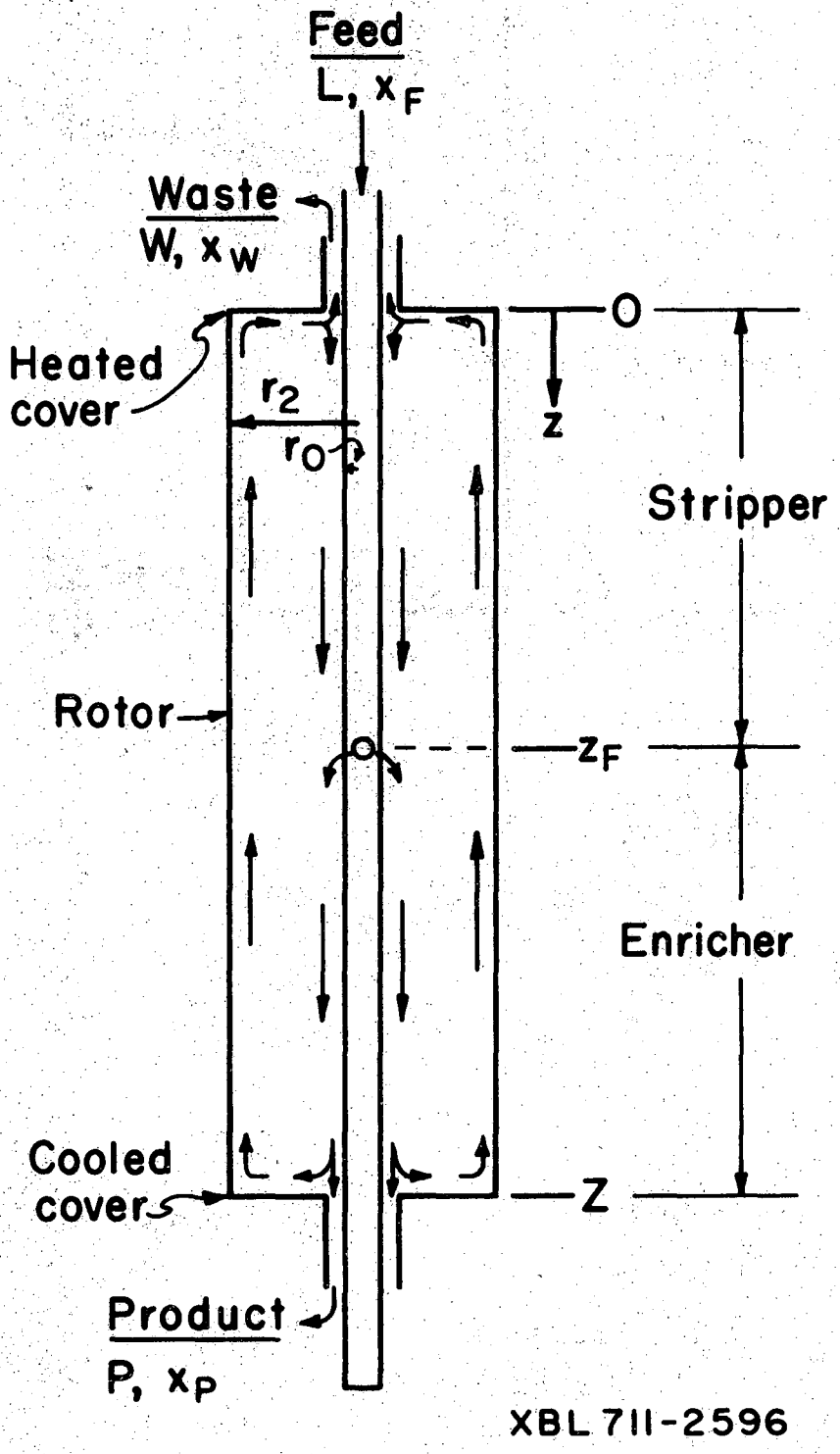
Feed
L, x_F
Waste
W, x_W
Heated cover
r_2
r_0
0
z
Stripper
Rotor
z_F
Enricher
Cooled cover
Z
Product
P, x_P
XBL 711-2596

Fig. 7

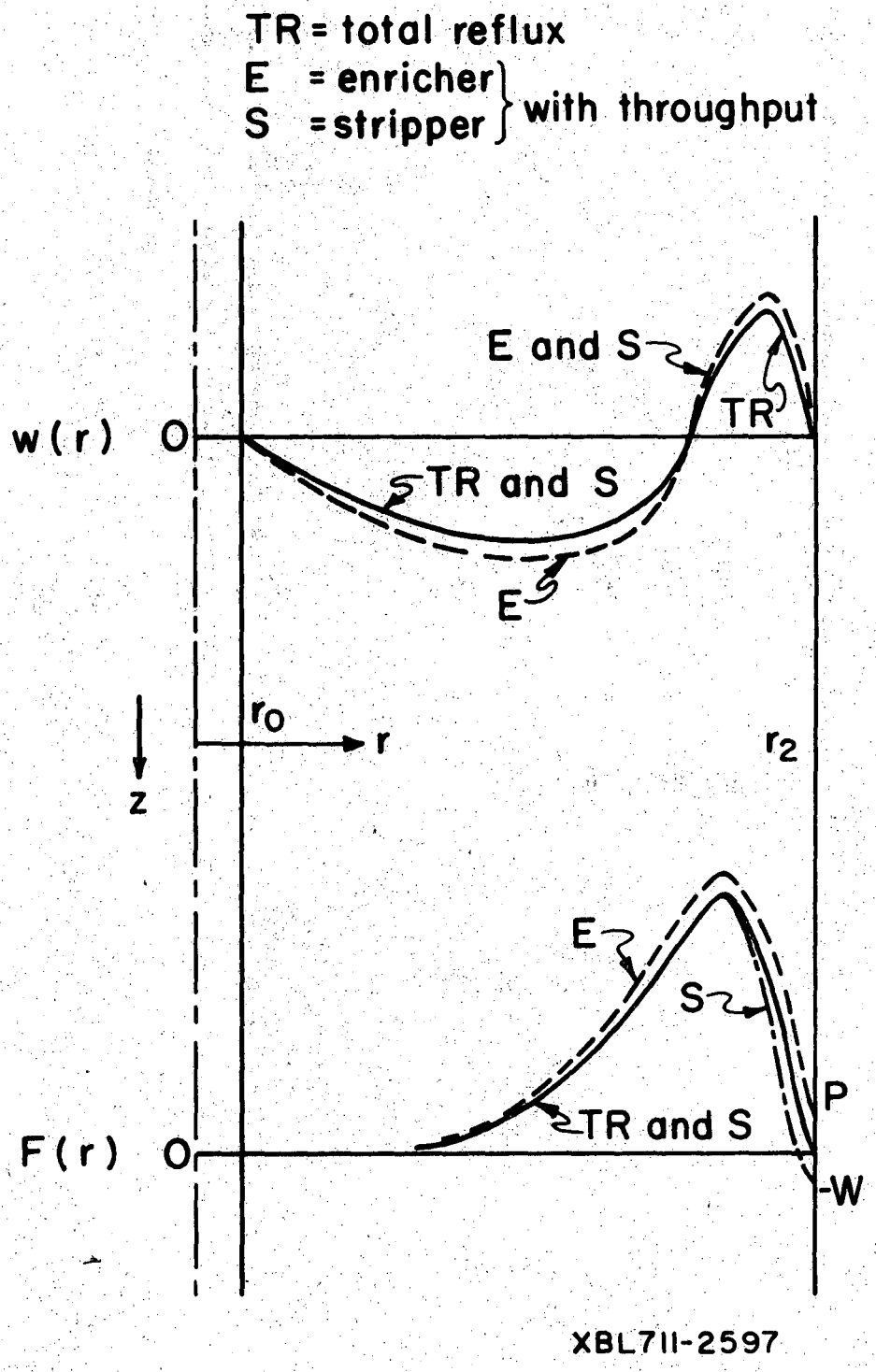
TR = total reflux
E = enricher
S = stripper
with throughput
E and S
TR
w(r)
O
TR and S
E
r0
r
r2
z
E
S
P
TR and S
F(r)
O
-W
XBL711-2597

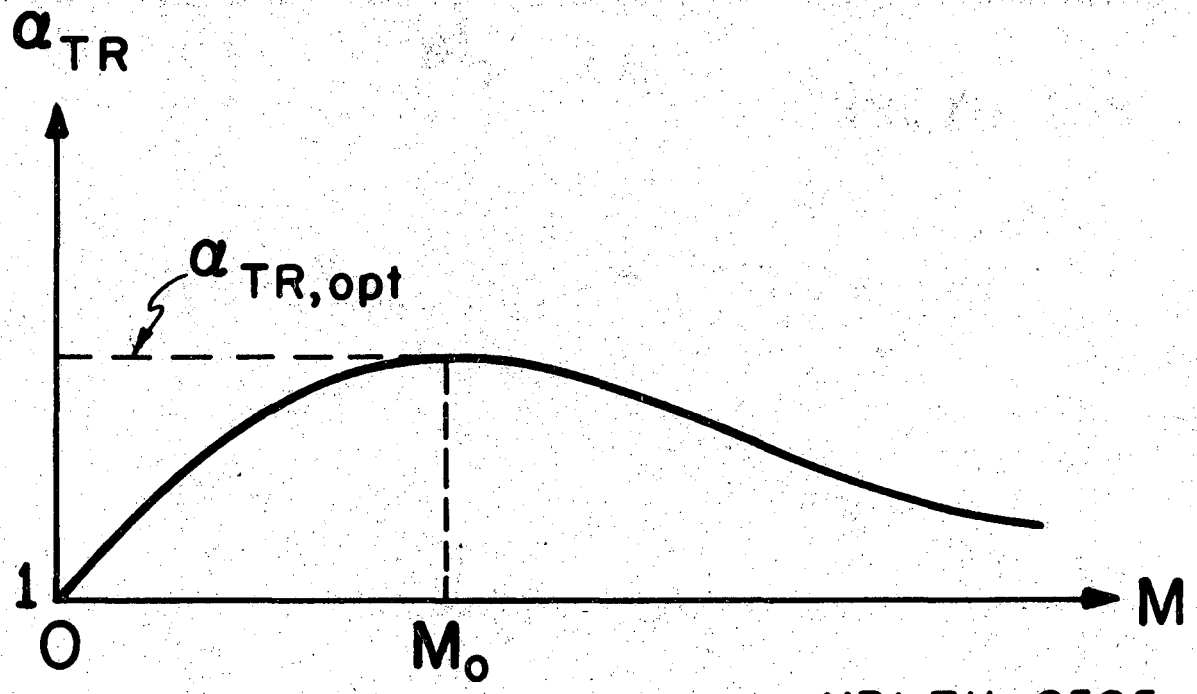

XBL711-2585

Fig. 9

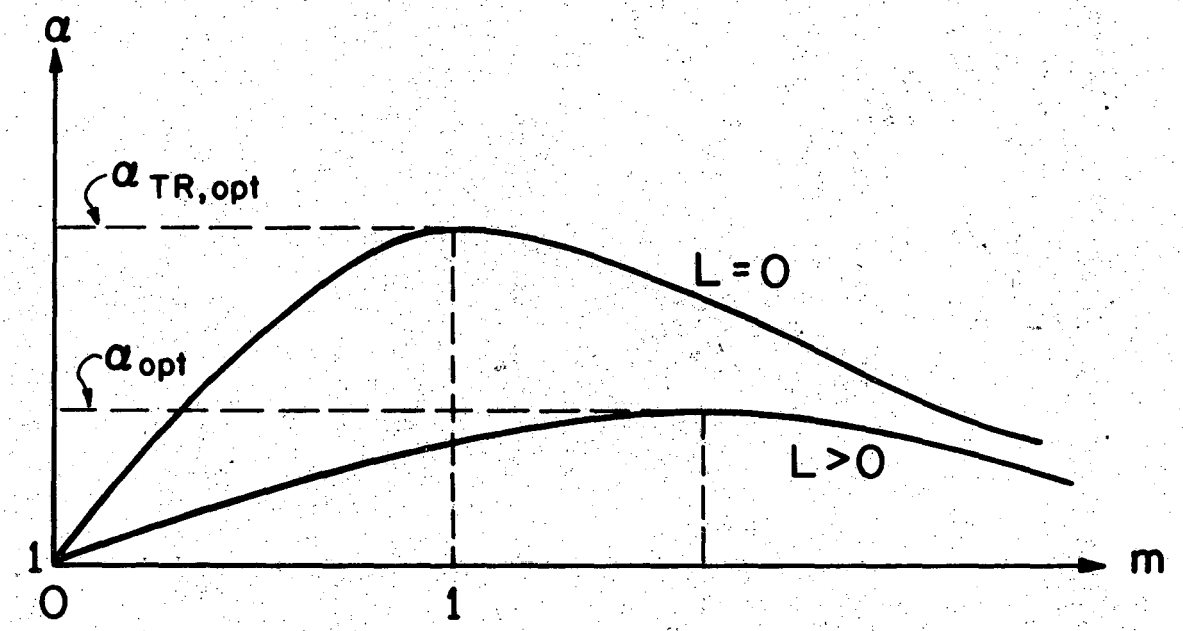

XBL711-2586

Fig. 10

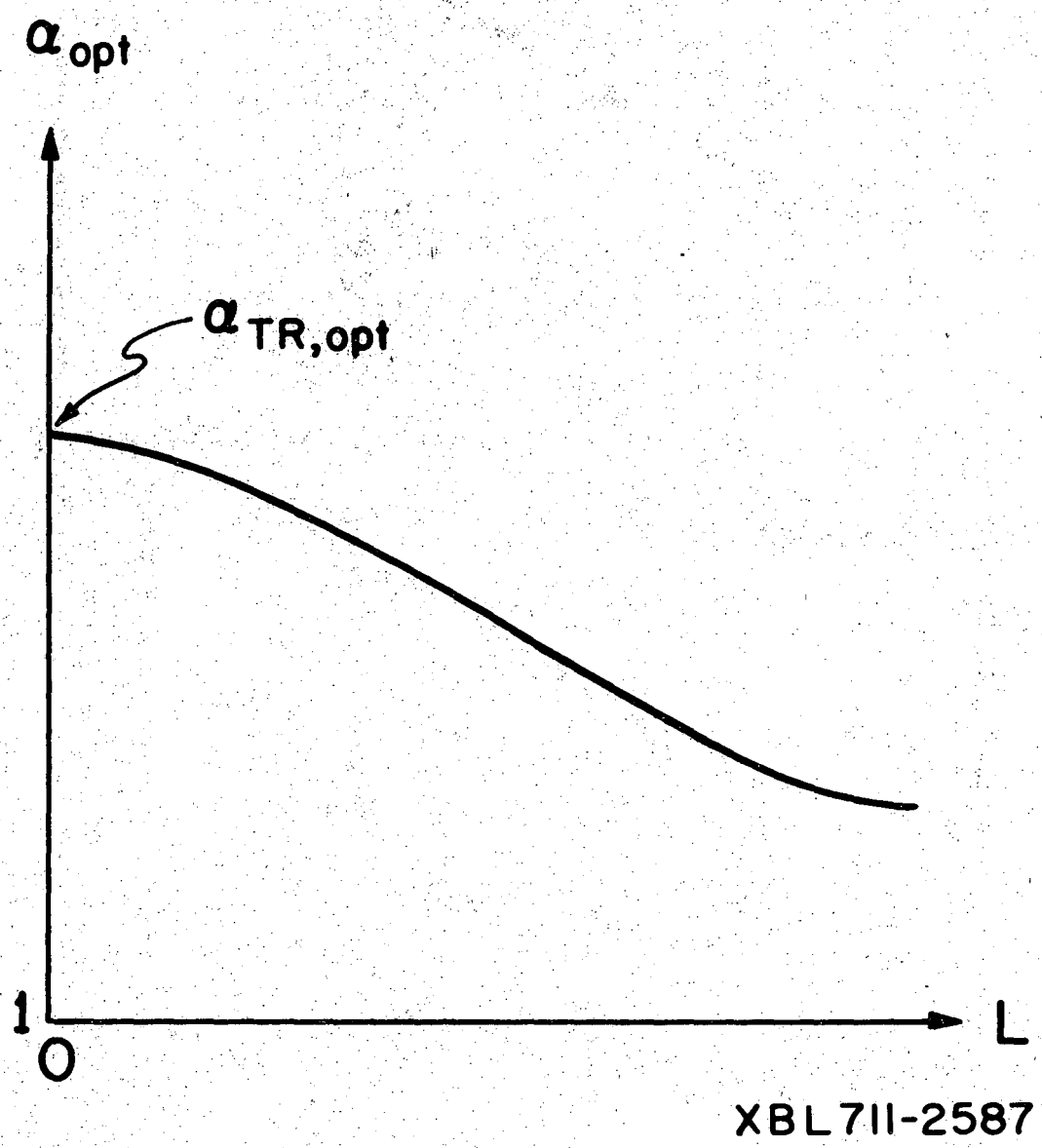

Fig. 11

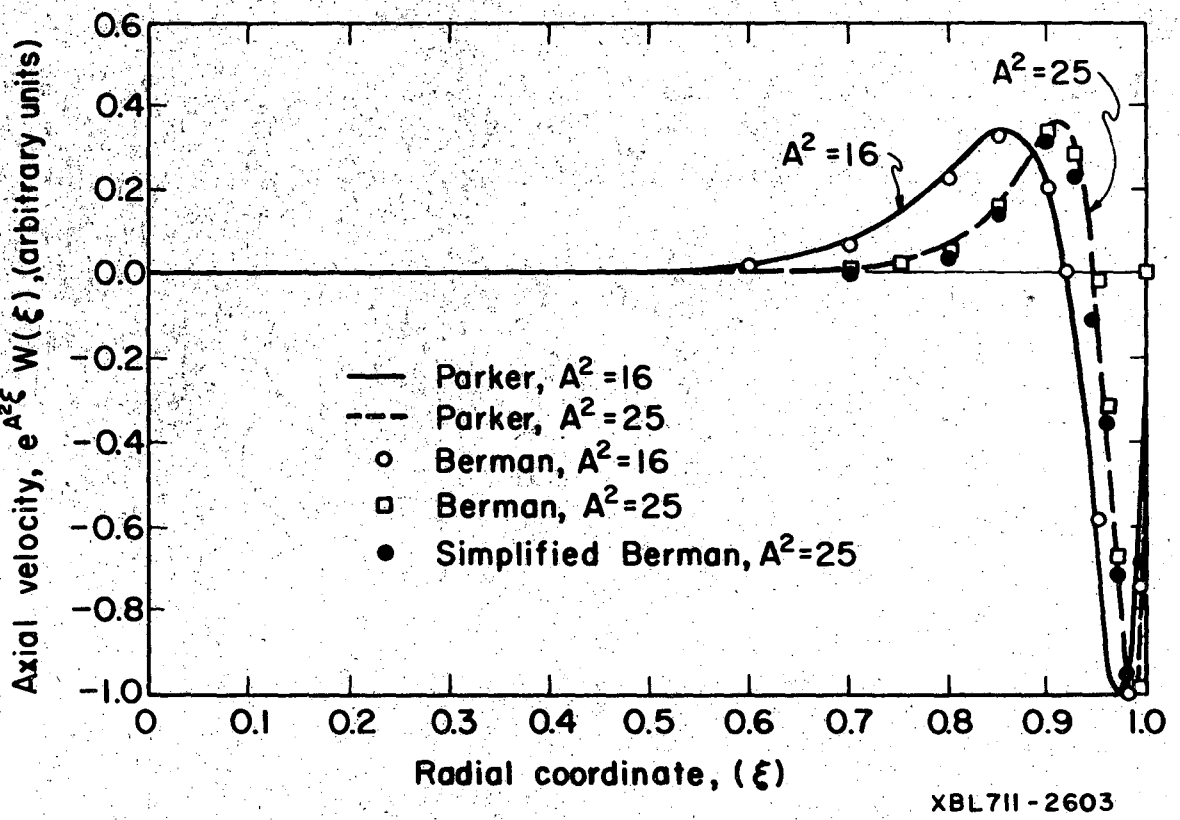
Axial velocity, $e^{A^2\xi}$ W(ξ), (arbitrary units)
Radial coordinate, (ξ)
A^2 = 25
A^2 = 16
Parker, A^2 = 16
Parker, A^2 = 25
Berman, A^2 = 16
Berman, A^2 = 25
Simplified Berman, A^2 = 25
0.6
0.4
0.2
0.0
-0.2
-0.4
-0.6
-0.8
-1.0
0
0.1
0.2
0.3
0.4
0.5
0.6
0.7
0.8
0.9
1.0
XBL711-2603

Fig. 12

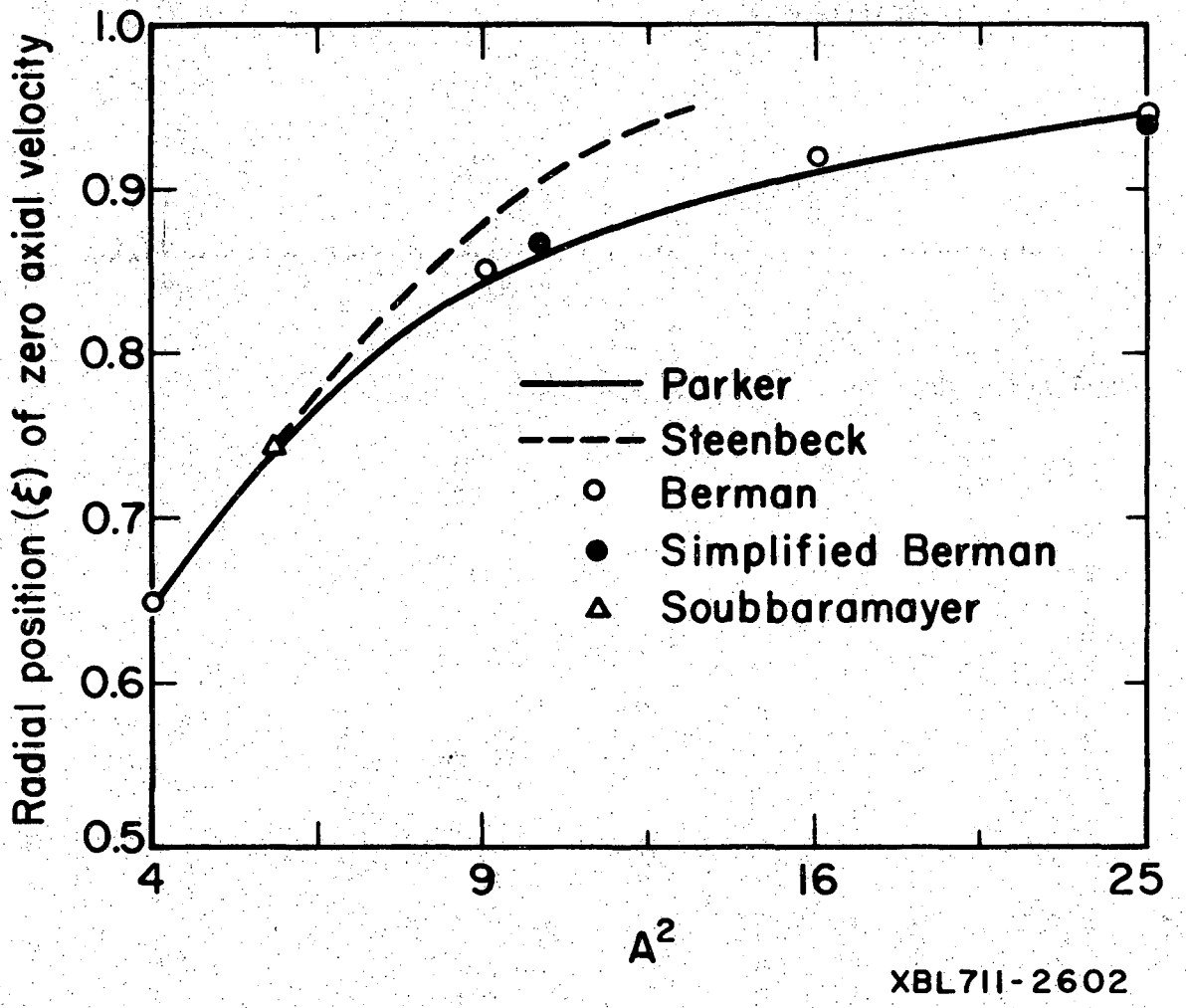
Radial position (ξ) of zero axial velocity
1.0
0.9
0.8
0.7
0.6
0.5
4
9
16
25
A²
Parker
Steenbeck
Berman
Simplified Berman
Soubbaramayer
XBL711-2602

Fig. 13

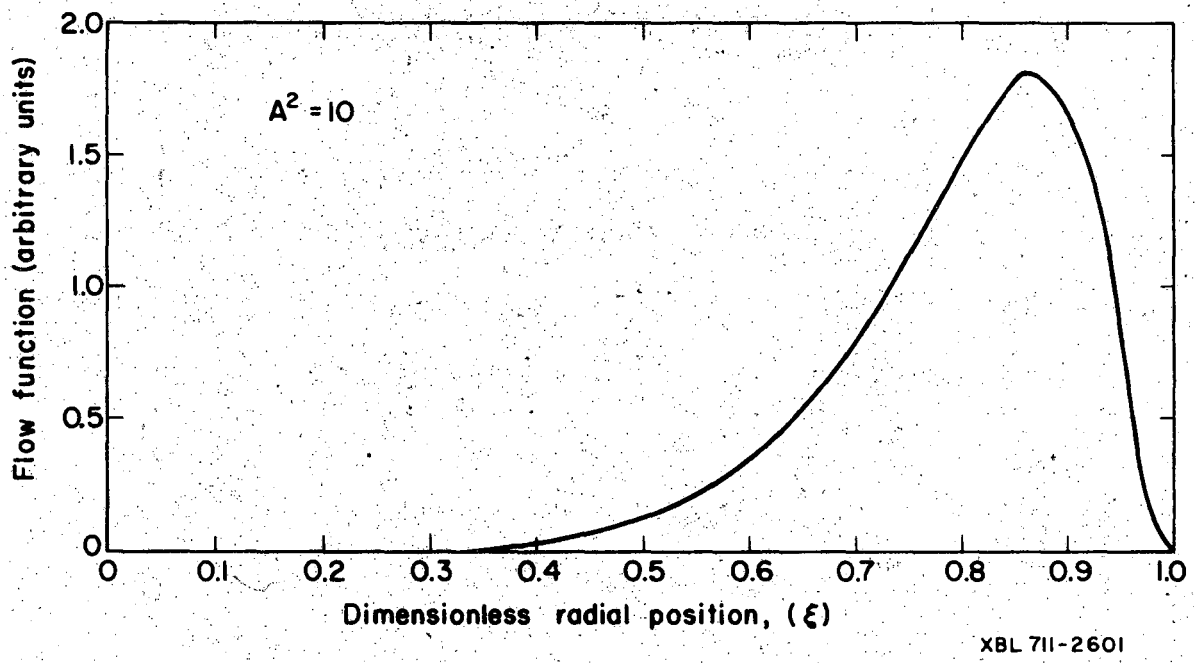
2.0
1.5
1.0
0.5
0
$A^2 = 10$
Flow function (arbitrary units)
0
0.1
0.2
0.3
0.4
0.5
0.6
0.7
0.8
0.9
1.0
Dimensionless radial position, (ξ)
XBL 711-2601

Fig. 14

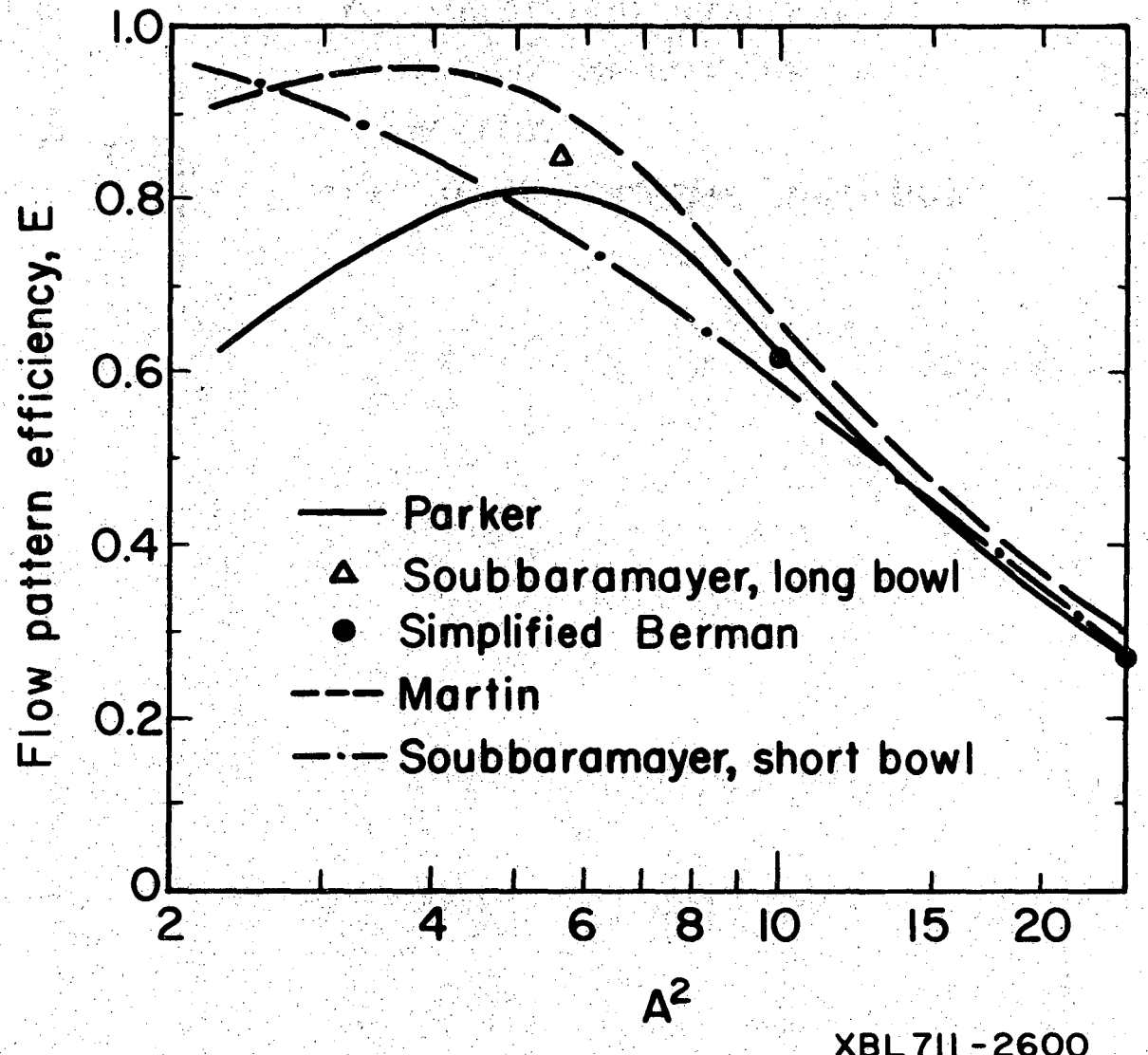
1.0
0.8
0.6
0.4
0.2
0
Flow pattern efficiency, E
2
4
6
8
10
15
20
A²
Parker
Soubbaramayer, long bowl
Simplified Berman
Martin
Soubbaramayer, short bowl
XBL 711-2600

Fig. 15

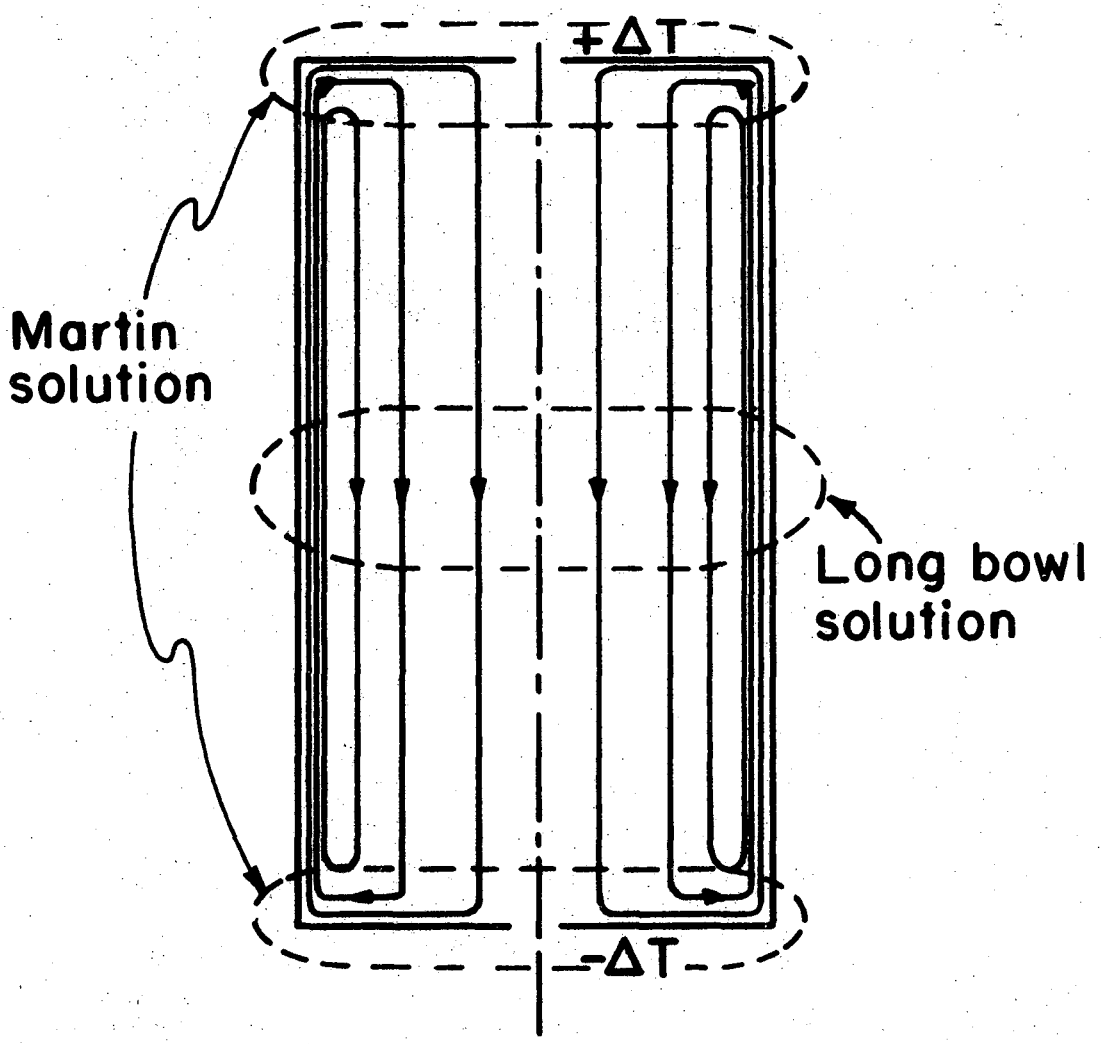

Fig. 16

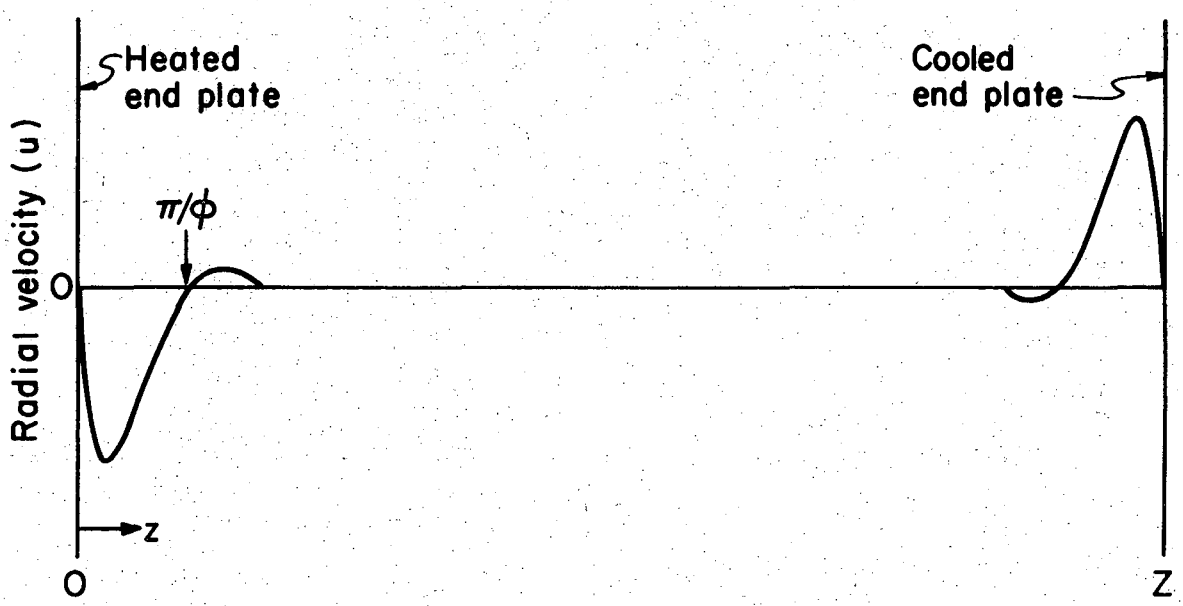
Heated
end plate
Cooled
end plate
Radial velocity (u)
π/ϕ
0
z
0
Z
XBL711-2598

Fig. 17

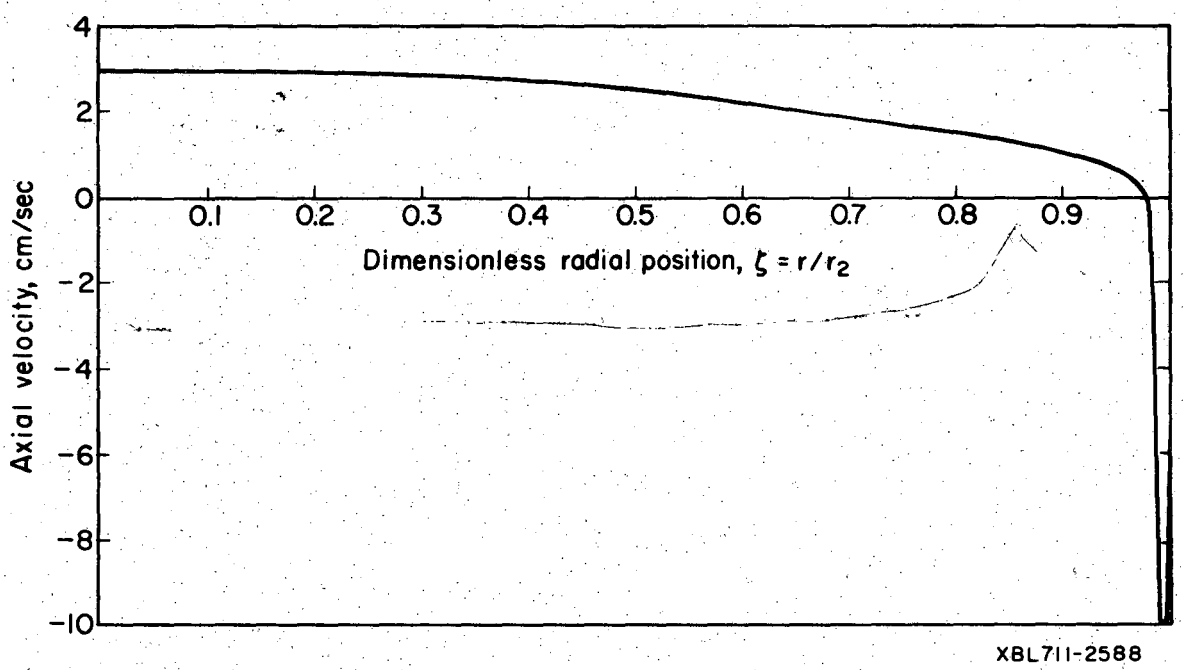
4
2
0
-2
-4
-6
-8
-10
0.1
0.2
0.3
0.4
0.5
0.6
0.7
0.8
0.9
Axial velocity, cm/sec
Dimensionless radial position, ζ = r/r2
XBL711-2588

Fig. 18

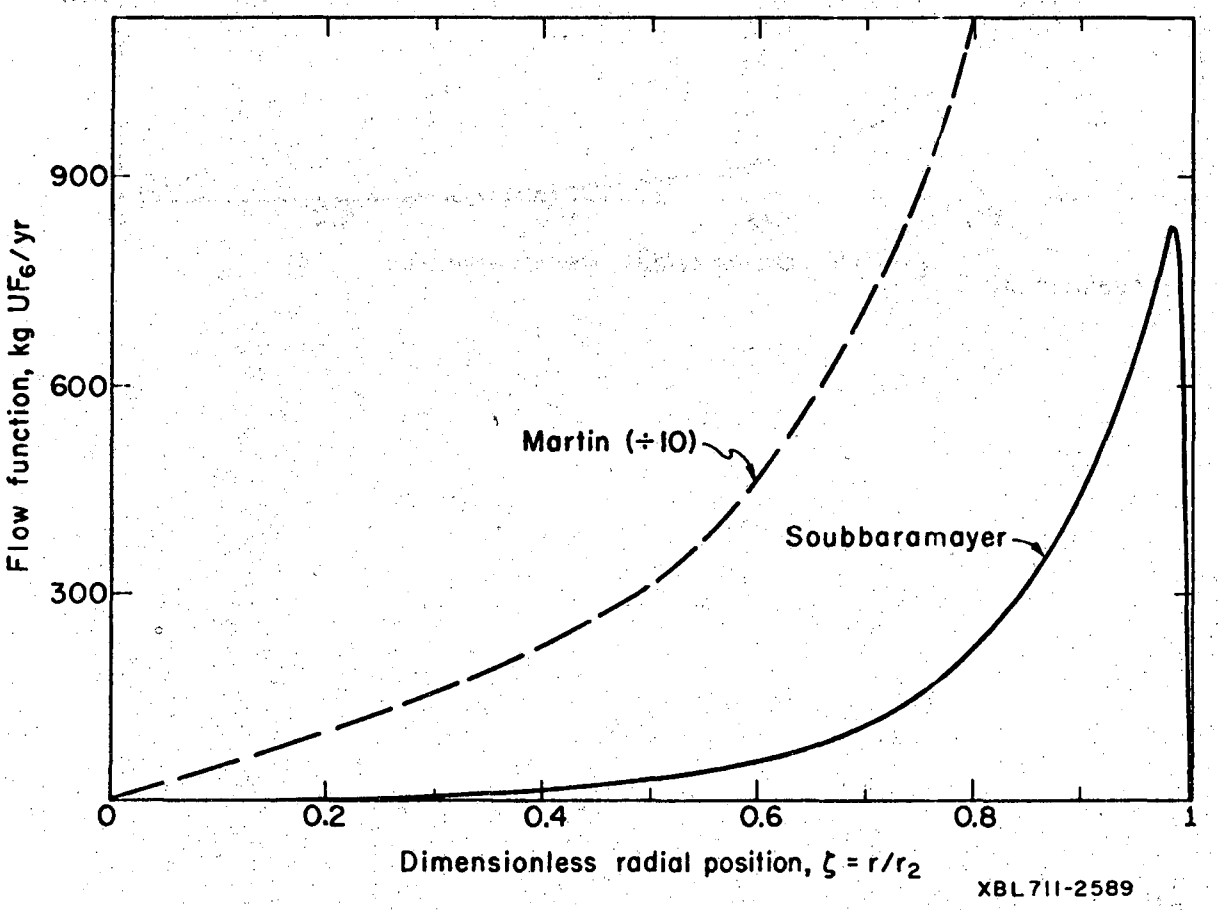
900
600
300
Flow function, kg UF_6/yr
Martin (÷10)
Soubbaramayer
0
0.2
0.4
0.6
0.8
1
Dimensionless radial position, $\zeta = r/r_2$
XBL711-2589

Fig. 19

TECHNICAL INFORMATION DIVISION
LAWRENCE RADIATION LABORATORY
UNIVERSITY OF CALIFORNIA
BERKELEY, CALIFORNIA 94720